HIV-1 blocks the signaling adaptor MAVS to evade antiviral host defense after sensing of abortive HIV-1 RNA by the host helicase DDX3

Gringhuis, Sonja I.; Hertoghs, Nina; Kaptein, Tanja M.; Zijlstra-Willems, Esther M.; Sarrami-Fooroshani, Ramin; Sprokholt, Joris K.; van Teijlingen, Nienke H.; Kootstra, Neeltje A.; Booiman, Thijs; van Dort, Karel A.; Ribeiro, Carla M. S.; Drewniak, Agata; Geijtenbeek, Teunis B. H.

Published in:
Nature immunology

DOI:
10.1038/ni.3647

Published: 01/01/2017

Document Version
Peer reviewed version

HIV-1 blocks MAVS signaling to evade antiviral host defense after sensing of abortive HIV-1 RNA by the helicase DDX3

Sonja I. Gringhuis[1*], Nina Hertoghs[1], Tanja M. Kaptein[1], Esther M. Zijlstra-Willems[1], Ramin Sarrami-Fooroshani[1], Joris K. Sprokholt[1], Nienke H. van Teijlingen[1], Neeltje A. Kootstra[1], Thijs Booiman[1], Karel A. van Dort[1], Carla M.S. Ribeiro[1], Agata Drewniak[1], and Teunis B.H. Geijtenbeek[1*]

[1]Department of Experimental Immunology, Academic Medical Center, University of Amsterdam, Meibergdreef 9, 1105 AZ Amsterdam,The Netherlands

* Corresponding authors:
S.I. Gringhuis, Ph.D.
Department of Experimental Immunology, Academic Medical Center, University of Amsterdam, Meibergdreef 9, 1105 AZ Amsterdam, The Netherlands; E-mail: s.i.gringhuis@amc.uva.nl; Tel: +31 20 56 67008.

T.B.H. Geijtenbeek, Ph.D.
Department of Experimental Immunology, Academic Medical Center, University of Amsterdam, Meibergdreef 9, 1105 AZ Amsterdam, Netherlands; E-mail: t.b.geijtenbeek@amc.uva.nl; Tel: +31 20 56 66063.

ABSTRACT

The mechanisms by which human immunodeficiency virus 1 (HIV-1) avoids immune surveillance by dendritic cells (DCs) and thereby prevents protective adaptive immune responses remain poorly understood. Here we show that HIV-1 actively arrested antiviral immune responses by DCs, which contributed to efficient HIV-1 replication in infected individuals. We identified the RNA helicase DDX3 as an HIV-1 sensor that bound abortive HIV-1 RNA upon HIV-1 infection and induced DC maturation, type I interferon and proinflammatory responses via MAVS. Notably, HIV-1 recognition by DC-SIGN activated the mitotic kinase PLK1, which suppressed signaling downstream of MAVS, thereby interfering with intrinsic host defense during HIV-1 infection. Finally, we show that PLK1-mediated suppression of DDX3-MAVS signaling was a viral strategy that accelerated HIV-1 replication in infected individuals.

Dendritic cells (DCs) are crucial in the induction of adaptive immune responses to human immunodeficiency virus 1 (HIV-1)[1]. However, DCs do not mount protective immunity against HIV-1[2], which is attributed to the ability of HIV-1 to escape immune surveillance.

DCs sense invading viruses through pattern recognition receptors (PRRs) that trigger type I interferon (IFN) and cytokine responses that lead to intrinsic antiviral defenses and adaptive immunity[1]. Type I IFNs IFN-α/IFN-β activate, via autocrine signaling, an antiviral program of IFN-stimulated genes (ISGs) that counteract virus replication[3-5]. However, type I IFNs also induce antiviral adaptive immunity via DC maturation[6] and T helper cell polarization[7]. Although HIV-1 infect DCs efficiently, neither DC activation nor type I IFN responses are induced[2]. Type I IFN responses early during infection lowers susceptibility to SIV in rhesus macaques and slows disease progression[8]. These observations strongly suggest that the absence of type I IFN responses underlie the lack of protective immunity during HIV-1 infection.

During the life cycle of HIV-1, various classes of host PRRs encounter different HIV-1 ligands that could potentially trigger type I IFN responses. C-type lectin receptor DC-SIGN recognizes HIV-1 envelope protein gp120, which triggers serine-threonine kinase Raf-1-dependent signaling[9,10]. Cytosolic receptor RIG-I recognizes purified HIV-1 ssRNA, but it remains unclear whether this interaction also occurs during infection[11]. TLR8 recognizes HIV-1 ssRNA upon endosomal degradation of virions, thereby inducing NF-κB activation[12]. HIV-1 exploits cooperative DC-SIGN and TLR8 signaling in DCs for transcription initiation and elongation[12]. NF-κB activation initiates transcription from the integrated provirus, however RNA polymerase is unable to proceed beyond the first 58 nucleotides, generating 'abortive' HIV-1 RNAs[12,13]. DC-SIGN-induced Raf-1 activation leads to recruitment of transcription elongation factor pTEF-b, which modulates RNA polymerase, and transcription proceeds to generate full-length functional HIV-1 transcripts that contain poly(A) tails[12].

These full-length transcripts remain unspliced or are processed into multiply or singly spliced transcripts; all are exported from the nucleus into the cytoplasm. Several DEAD box RNA helicases related to RIG-I, such as DDX1, DDX3 and DDX5, assist in their nuclear export[14,15]. DDX3 is also involved in translation of HIV-1 transcripts via direct binding to the 5'm^{7}GTP cap structure of HIV-1 transcripts[16], and forming a translation initiation complex consisting of DDX3 with elongation factor eIF4G and poly(A)-binding protein (PABP), as well as elongation factor eIF4A[16,17]. This complex allows 43S ribosomal units to attach to the transcripts and ultimately *de novo* synthesis of viral proteins[16,17]. HIV-1 cDNA, generated during reverse transcription, is recognized by DNA sensor cyclic GMP-AMP synthase (cGAS), which, via adaptor protein STING, leads to activation of transcription factor IRF3 that drives IFN-β expression[18,19]. HIV-1 escapes detection by cGAS by limiting viral DNA via host proteins such as cytosolic exonuclease TREX1, which digest HIV-1 DNA[20], and phosphohydrolase SAMHD1, which limits generation of HIV-1 DNA[21]. However, SAMHD1-mediated restriction of DC infection does not account for lack of DC activation[22]. Thus, while viral RNA, DNA and proteins are recognized by various host proteins, it remains unclear how HIV-1 avoids immune surveillance in DCs.

Here we identified RNA helicase DDX3 as a sensor for abortive HIV-1 RNA in DCs, which induced type I IFN responses and DC maturation via the adaptor protein MAVS. However, simultaneous recognition of HIV-1 by DC-SIGN suppressed these responses via Raf-1-mediated activation of host factor PLK1, which impeded signaling downstream of MAVS (**Supplementary Fig. 1**). The identification of a rare dual MAVS(Q198K-S409F) mutant that is resistant to PLK1 inactivation, thereby contributing to limiting the viral RNA load, demonstrated the significance of DDX3-mediated sensing for HIV-1 replication in infected individuals.

RESULTS

HIV-1 innate signaling via Raf-1 blocks type I IFN responses

As HIV-1 activates Raf-1[12], we investigated whether Raf-1 is involved in suppression of type I IFN responses after HIV-1 infection of human DCs. Monocyte-derived DCs (moDCs) did not express *IFNB* mRNA after infection with laboratory R5-tropic strain HIV-1_{BaL} but Raf-1 inhibition with small molecule inhibitor GW5074 or silencing of Raf-1 expression by RNA interference (RNAi) induced transient expression of *IFNB* transcripts that peaked at 4 h post-infection, as well as mRNA expression of various ISGs, such as *ISG15*, *MX2*, *TRIM5*, *TRIM22*, and *APOBEC3G* (**Fig. 1a-c**). GW5074 did not diminish TLR4-induced *IFNB* expression in moDCs (**Supplementary Fig. 2**). HIV-1_{BaL} infection induced *IFNB* expression only in GW5074-treated but not untreated human primary myeloid, dermal, intestinal and vaginal DCs isolated from blood, skin, intestinal and vaginal tissues (**Fig. 1d**). We also observed *IFNB* expression after infection of GW5074-treated moDCs both with different laboratory strains, i.e. R5-tropic HIV-1_{SF162} or X4-tropic HIV-1_{R9} and HIV-1_{LAI}, and primary R5-tropic HIV-1 strains isolated from infected patients (**Fig. 1f**). These data indicate that Raf-1 activation following HIV-1 infection in DCs blocks antiviral type I IFN responses.

HIV-1 infection triggers type I IFN responses via DDX3

Induction of *IFNB* expression in GW5074-treated HIV-1_{BaL}-infected moDCs was abrogated by the nucleoside analog reverse-transcriptase inhibitor azidothymidine (AZT) or the integrase inhibitor raltegravir, and by silencing TLR8 by RNAi (**Fig. 2a**). Because TLR8 triggering by HIV-1 ssRNA is crucial to HIV-1 transcription initiation[12], and because HIV-1 ssRNA did not induce IFN-β directly (**Fig. 2a**), these data suggest that type I IFN responses were triggered by HIV-1 RNA transcripts. Silencing of cDNA sensor cGAS and its downstream effector STING[18,19] abrogated *IFNB* expression in TREX1-silenced but not in

GW5074-treated moDCs upon HIV-1_{BaL} infection (**Fig. 2b** and **Supplementary Fig. 3**). GW5074 treatment enhanced *IFNB* expression in TREX1-silenced HIV-1_{BaL}-infected moDCs, which was partially inhibited by cGAS silencing and completely by AZT but not raltegravir (**Fig. 2b** and **Supplementary Fig. 3**). Thus, there are at least two independent HIV-1 sensing pathways in DCs: a Raf-1-sensitive pathway triggered by an RNA sensor after HIV-1 transcription and the TREX1-sensitve pathway induced by DNA sensor cGAS after reverse transcription.

To identify the RNA sensor, we silenced RIG-I and MDA5, which did not interfere with *IFNB* expression in GW5074-treated HIV-1_{BaL}-infected moDC (**Supplementary Fig. 3**). Silencing of DDX3 but not DDX1 or DDX5 by RNAi abrogated *IFNB* expression in GW5074-treated but not in TREX1 silenced moDCs upon HIV-1_{BaL} infection (**Fig. 2c and Supplementary Fig. 3**). DDX3 silencing in moDCs did not affect RIG-I-MDA5-, cGAS-STING- or TLR4-induced *IFNB* expression (**Supplementary Fig. 3**). Rescue of DDX3 expression by plasmid transfection restored *IFNB* expression in DDX3-silenced GW5074-treated HIV-1_{BaL}-infected moDCs (**Fig. 2d**), excluding off-target silencing effects. We next examined whether DDX3 signals via MAVS, similar to other RNA sensors[18]. MAVS silencing inhibited *IFNB* expression in GW5074-treated HIV-1_{BaL}-infected moDCs (**Fig. 2e**), which was restored by transfection of MAVS plasmid (**Fig. 2f**). Furthermore, MAVS co-immunoprecipitated with DDX3, and vice versa, from whole cell extracts of both untreated and GW5074-treated HIV-1_{BaL}-infected moDCs, but not of uninfected moDCs (**Fig. 2g**). Confocal microscopy showed that HIV-1 infection invoked partial colocalization of DDX3 around mitochondria (**Fig. 2h**).

In contrast to moDCs, HIV-1_{BaL} infection induced *IFNB* expression in monocyte-derived macrophages that was further enhanced by GW5074 treatment, and abrogated after silencing of DDX3 or MAVS (**Fig. 2i**). We next examined whether other retroviruses also trigger

DDX3. HTLV-1, despite infection of moDCs (**Supplementary Fig. 2**), did not induce *IFNB* responses in either untreated or GW5074-treated moDCs (**Fig. 2j**). In contrast, HIV-2 infection induced *IFNB* expression in GW5074-treated moDCs, which was abrogated after silencing of DDX3 or MAVS (**Fig. 2j and Supplementary Fig 2**). These results imply that DDX3 not only triggers type I IFN responses through MAVS in DCs but also macrophages after HIV-1 infection, which are (partially) blocked by a Raf-1-mediated pathway.

DDX3 binding to abortive HIV-1 RNA leads to MAVS activation

Considering its role in HIV-1 translation[16,17], we next investigated whether DDX3 associates with MAVS within translation initiation complexes. Translation initiation complexes were retained on m^7GTP-agarose from whole cell extracts and analyzed by immunoblotting; DDX3, but not MAVS, associated with eIF4G, eIF4A and PABP within translation initiation complexes in HIV-1_{BaL}-infected but not uninfected moDCs (**Fig. 3a**). This result implies that the DDX3 fraction in translation initiation complexes is distinct from the fraction involved in MAVS-dependent signaling. Next, RNA immunoprecipitation (RIP) and re-RIP analyses showed that DDX3 together with eIF4G, but not MAVS, interacted with Tat-Rev mRNA in HIV-1_{BaL}-infected moDCs (**Fig. 3b**). Silencing of DDX3 but not MAVS by RNAi in moDCs blocked association of eIF4G to Tat-Rev transcripts (**Fig. 3c**). In contrast, DDX3-MAVS but not DDX3-eIF4G complexes bound abortive HIV-1 RNAs in HIV-1_{BaL}-infected moDCs (**Fig. 3b**). DDX3 silencing abrogated MAVS recruitment to abortive HIV-1 RNAs, while MAVS silencing did not interfere with the DDX3-abortive HIV-1 RNA association (**Fig. 3c**), suggesting that DDX3 sensing of abortive HIV-1 RNAs precedes DDX3 association with MAVS.

Next we transfected moDCs with different HIV-1-derived RNAs, thereby bypassing *IFNB* suppression by DC-SIGN. Transfection of moDCs with abortive HIV-1 RNAs (cap-TAR) induced *IFNB* expression, which was abrogated by silencing of DDX3 or MAVS (**Fig. 3d**). Activation of DC-SIGN using cross-linking antibodies abrogated *IFNB* expression in cap-TAR-transfected moDCs, while GW5074 treatment restored these responses (**Fig. 3e**). Notably, transfection of moDCs with Tat transcripts lacking their 3'poly(A) tail (cap-Tat) but not intact transcripts (cap-Tat-poly(A)) induced *IFNB* expression, which was abrogated by silencing of DDX3 or MAVS (**Fig. 3f**). DDX3 also binds some endogenous transcripts, such as β-globin mRNA[16]. Transfection of moDCs with β-globin transcripts lacking their 3'poly(A) tail (cap-β-globin) but not intact β-globin transcripts (cap-β-globin-poly(A)) induced *IFNB* expression, which was abrogated by silencing of DDX3 or MAVS (**Fig. 3f**). These results suggest that DDX3 binding of defective RNAs lacking the 3'poly(A) tail are recruited to MAVS and trigger type I IFN responses. independent of the (viral) nature of the RNA.

We next generated 293T cell lines that were depleted of either DDX3 (293TΔDDX3) or MAVS (293TΔMAVS) using CRISPR/Cas9-directed genome editing (**Supplementary Fig. 4**). Transfection of control 293T cells as well as 293TΔRIG-I, 293TΔMDA5 and 293TΔRIG-I-MDA5 cells but not 293TΔDDX3 or 293TΔMAVS cells with cap-TAR RNA induced *IFNB* expression (**Fig. 3g**). The RIG-I-MDA5 ligand poly(I:C)-LyoVec induced *IFNB* expression in control 293T and 293TΔDDX3 cells but not 293TΔRIG-I, 293TΔMDA5, 293TΔRIG-I-MDA5 or 293TΔMAVS cells (**Fig 3g**). Thus, the DDX3-MAVS sensing mechanism is not restricted to DCs.

DDX3 activates IRF3 via TRAF3 recruitment to MAVS

RIG-I and MDA5 induce recruitment of TRAF3 to MAVS aggregates, which activate TBK1 and IKKε to recruit IRF3 to MAVS and phosphorylate IRF3 at Ser396[18,23,25]. TRAF3 silencing abrogated *IFNB* expression in GW5074-treated HIV-1_{BaL}-infected moDCs (**Fig. 4a**). TRAF3 co-immunoprecipitated with DDX3 from GW5074-treated but not untreated HIV-1_{BaL}-infected moDC whole cell extracts, which was abrogated by MAVS silencing (**Fig. 4b**). These results imply that Raf-1 impedes recruitment of TRAF3 to MAVS upon HIV-1 infection.

Silencing of IRF3 or both TBK1 and IKKε abrogated *IFNB* expression in GW5074-treated HIV-1_{BaL}-infected moDCs (**Fig. 4c**). FACS analyses showed that HIV-1_{BaL} infection of GW5074-treated moDCs induced phosphorylation of TBK1 and IKKε at Ser172, a mark of activation[24], which was abrogated by silencing of DDX3 or MAVS (**Fig. 4d**). Nuclear translocation and phosphorylation of IRF3 in GW5074-treated HIV-1_{BaL}-infected moDCs was abrogated by silencing of DDX3 or MAVS (**Fig. 4e**). Recruitment of IRF3 to DDX3, as assessed by co-immunoprecipitation from GW5074-treated HIV-1_{BaL}-infected moDC whole cell extracts, was attenuated by silencing MAVS, TRAF3 or TBK1-IKKε (**Fig. 4b**). These results indicate that sensing of abortive HIV-1 RNA by DDX3 leads to MAVS-TRAF3- and TBK1-IKKε-dependent activation of IRF3 upon Raf-1 inhibition.

HIV-1-activated PLK1 impedes TRAF3 recruitment to MAVS

Association of mitotic kinase PLK1 with MAVS blocks MAVS-TRAF3 interactions[26]. Notably, PLK1 silencing induced transient *IFNB* expression in untreated HIV-1_{BaL}-infected moDCs (**Fig. 5a,b**), similar to that observed in GW5074-treated moDCs (**Fig. 1a,b**). PLK1 silencing in HIV-1_{BaL}-infected moDCs did not abrogate Tat-Rev mRNA induction (**Supplementary Fig. 5**), indicating that PLK1, unlike Raf-1, is not involved in HIV-1 transcription elongation[12]. PLK1 co-immunoprecipitated with DDX3 from whole cell extracts

of HIV-1_{BaL}-infected but not uninfected moDCs, which was abrogated by silencing MAVS and GW5074 treatment(**Fig. 5c)**. Both TRAF3 and IRF3 co-immunoprecipitated with DDX3 in PLK1-silenced HIV-1_{BaL}-infected moDCs (**Fig. 5d** and **Supplementary Fig. 6**). These results indicate that Raf-1 activation induces association of PLK1 with MAVS in HIV-1-infected DCs, preventing downstream DDX3-MAVS signaling.

PLK1 resides in an inactive state due to intramolecular interactions, which are released when PLK1 becomes phosphorylated at Thr210, enabling PLK1 to bind its substrates, like MAVS[27,28]. FACS analyses showed that both HIV-1_{BaL} infection and stimulation with gp120 of moDCs induced PLK1 phosphorylation at Thr210, which was abrogated by blocking antibodies against DC-SIGN or GW5074 (**Fig. 5e,f**), indicating that HIV-1_{BaL} induces Raf-1 activation and subsequent PLK1-Thr210 phosphorylation via DC-SIGN.

Recombinant Raf-1 did not phosphorylate Flag-PLK1 at Thr210 in a biochemical assay, in contrast to recombinant protein kinase A, used as a control (**Fig. 5g**), suggesting that PLK1 is not a direct target of Raf-1. Ste20-like kinases have been reported to phosphorylate PLK1 at Thr210[29]. As Ste20-like kinase MST1 interacts with adaptor protein CNK1[30] that is a component of the Raf-1 signalosome attached to DC-SIGN in resting DCs[10], we assessed whether PLK1 is a target of MST1. Recombinant MST1 phosphorylated Flag-PLK1 at Thr210 (**Fig. 5g**). MST1 was transiently activated in HIV-1_{BaL}-infected moDCs, which was abrogated by blocking antibodies against DC-SIGN or GW5074 (**Fig. 5h**) as activity of MST1 was measured after immunoprecipitation from moDCs in a kinase activity assay. GW5074-sensitive MST1 activity after HIV-1_{BaL} infection or gp120 stimulation coincided with MST1 phosphorylation at its autophosphorylation site Thr183[31] in moDCs, as assessed by FACS analyses (**Fig. 5i**). Silencing of MST1 by RNAi in HIV-1_{BaL}-infected moDCs abrogated both PLK1 phosphorylation (**Fig. 5j**) and co-immunoprecipitation of PLK1 with DDX3 from whole cell extracts (**Fig. 5k**), while inducing TRAF3 and IRF3 co-immunoprecipitation with

DDX3 (**Fig. 5k**), IRF3 activation (**Supplementary Fig. 6**) and *IFNB* expression (**Fig. 5l**). Similar to Raf-1 inhibition, MST1 silencing blocked expression Tat-Rev mRNA expression in HIV-1_{BaL}-infected moDCs (**Supplementary Fig. 2**), suggesting that MST1 is involved in HIV-1 transcription elongation. Together, these data indicate that HIV-1 binding to DC-SIGN triggers Raf-1-dependent MST1 activation, which leads to PLK1 phosphorylation and binding to MAVS, thus blocking DDX3-MAVS signaling.

Type I IFN responses suppress HIV-1 replication

We investigated the effect of type I IFN responses on HIV-1 replication in DCs. FACS analyses showed that blocking antibodies against the IFN-α/β receptor (IFNR) did not affect the % of moDCs that expressed the viral protein p24 after HIV-1_{BaL} infection (**Fig. 6a**). Silencing of PLK1 by RNAi lowered the % of $p24^+$ moDCs after HIV-1_{BaL} infection, whereas blocking IFNR antibodies enhanced infection to levels similar to control-silenced moDCs (**Fig. 6a**), indicating that HIV-1 suppresses IFN-β through PLK1 to efficiently infect moDCs.

We next analyzed the effect of single nucleotide polymorphisms (SNP) in MAVS within a human MSM ('men who have sex with men') cohort of untreated HIV-1-infected individuals. We identified three SNPs within *MAVS* that showed significant differences in plasma viral load, rs7262903, rs7269320 and rs7267297. rs7262903 and rs7269320 result in amino acid substitutions within MAVS (Gln198Lys (Q198K), Ser409Phe (S409F)), whereas rs7267297 lies within the 3'UTR of *MAVS*. rs7262903 and rs7269320 were 100% linked within the MSM cohort (n = 6); linkage disequilibrium in the global population is D' = 0.956, $r^2 = 0.559$ (HapMap release 23). Plasma viral load at set point was significantly lower in HIV-1-infected individuals homozygous for the minor alleles of rs7262903/rs7269320 (minor genotype), compared to individuals homozygous for the major alleles (major genotype) ($p1 = 0.044$; Student's *t*-test), while no differences were detected between individuals with heterozygous

and major genotypes ($p2 = 0.215$; Student's *t*-test) (**Fig. 6b**). We observed a significant delay in the time from seroconversion to viral RNA load > $10^{4.5}$ copies/ml plasma ($p1 = 0.025$, RH = 0.106, 95% CI 0.015-0.759; Cox regression), which was the median HIV-1 RNA load in the used cohort[32], in minor genotype individuals compared with major genotype individuals (**Fig. 6c**). Minor genotype individuals showed no significant effect on disease progression (AIDS according to the CDC definition 1993), followed over 180 months, likely due to the low number of individuals with this genotype (6/304) within the MSM cohort (data not shown). These data indicate that the DDX3-MAVS pathway is important in controlling HIV-1 replication, not only during the acute infection but also the clinical latency stage.

We next examined the effect of MAVS(Q198K-S409F) protein, encoded by minor genotype alleles, on HIV-1 replication in DCs from healthy donors. HIV-1_{BaL} infected a lower % of $p24^+$ moDCs derived from healthy minor genotype individuals (minor genotype moDCs), compared to major genotype moDCs, whereas blocking IFNR antibodies enhanced infection to levels similar to major genotype moDCs (**Fig. 6d**), indicating that HIV-1 does not suppress type I IFN responses in DCs expressing MAVS(Q198K-S409F).

Both major and minor genotype moDCs responded similarly to RIG-I-MDA5 ligands, such as poly(I:C)-LyoVec or measles virus, in the induction of *IFNB* expression (**Fig. 7a**), indicating that MAVS(Q198K-S409F) is functionally neutral, as reported for MAVS(Q198K)[33]. HIV-1_{BaL} infection induced *IFNB* and ISG expression in both untreated and GW5074-treated minor genotype moDCs, in contrast to heterozygous genotype moDCs that only induced *IFNB* expression after GW5074 treatment (**Fig. 7b,c**), like major genotype moDCs (**Fig. 1a**). We also observed *IFNB* expression after HIV-1_{BaL} infection of both untreated and GW5074-treated primary dermal DCs isolated from healthy minor genotype individuals (**Fig. 7d**). *IFNB* expression in HIV-1_{BaL}-infected minor genotype moDCs was abrogated by silencing of DDX3 or MAVS (**Fig. 7e**). Transfection of wild-type MAVS plasmid in MAVS-silenced

minor genotype moDCs rescued *IFNB* responses only after GW5074 treatment upon HIV-1_{BaL} infection (**Supplementary Fig. 7**), indicating that the identified MAVS SNPs mediated the observed effects. DDX3 co-immunoprecipitated with MAVS and TRAF3, but not PLK1, from HIV-1_{BaL}-infected minor genotype moDC whole cell extracts (**Fig. 7f**). Also, PLK1 silencing by RNAi did not affect *IFNB* expression in HIV-1_{BaL}-infected minor genotype moDCs (**Fig. 7g**). FACS analyses showed that Thr210 phosphorylation of PLK1 was normally induced by HIV-1_{BaL} in minor genotype moDCs (**Fig. 7h**). As Thr210-phosphorylated Flag-PLK1 immunoprecipitated MAVS from lysates of major genotype but not minor genotype moDCs (**Fig. 7i**), we investigated whether either Q198K or S409F or both mutations in MAVS are required to block PLK1-MAVS interactions. HIV-1_{BaL} infection induced *IFNB* expression in MAVS-silenced moDCs complemented with either MAVS(Q198K), MAVS(S409F) or MAVS(Q198K-S409F) by plasmid transfection, unlike the control-silenced moDCs that still expressed wild-type MAVS (**Fig. 7j**).

Similar to HIV-1_{BaL}, infection of moDCs with VSV-G-pseudotyped HIV-1 (HIV-1_{VSV-G}) does not result in type I IFN responses[34,35]. During HIV-1_{VSV-G} infection, retroviral integration and transcription initiation occur in a similar timeframe as HIV-1_{BaL}, however the VSV-G envelope does not bind DC-SIGN[12]. Infection of minor MAVS genotype but not major genotype moDCs with HIV-1_{VSV-G} induced *IFNB* expression 4 h post-infection (**Fig. 7k**), which was abrogated by DDX3 silencing (**Fig. 7k**), indicating that HIV-1_{VSV-G}-induced PLK1-mediated inhibition of MAVS signaling independent of DC-SIGN. Thus, PLK1 activated by both HIV-1 and VSV-G associates with MAVS, which suppresses IFN-β expression in moDCs, whereas both both Q198 and S409 in MAVS(Q198K-S409F) render MAVS insensitive to PLK1, allowing type I IFN responses.

Attenuation of DDX3-MAVS signaling suppresses immune activation

We next addressed whether suppression of DDX3-MAVS signaling prevents DC activation in response to HIV-1 infection. FACS analyses showed enhanced expression of maturation markers CD80, CD83 and CD86 in GW5074-treated but not untreated HIV-1_{BaL}-infected moDCs, which was abrogated by blocking antibodies against IFNR and silencing of DDX3 or MAVS by RNAi (**Fig. 8a,b**). In contrast, HIV-1_{BaL} infection of PLK1-silenced or minor MAVS genotype moDCs induced expression of these maturation markers even without GW5074 treatment, which was inhibited by blocking IFNR antibodies (**Fig. 8b,c**), indicating that innate type I IFN responses during HIV-1 infection induce DC maturation, which is blocked by HIV-1. Thus, HIV-1 targets DDX3-MAVS signaling not only to block antiviral responses, but also adaptive immune responses.

DISCUSSION

HIV-1 avoids immune surveillance required for the mounting of protective responses. Here we identified the RNA helicase DDX3 as an intracellular sensor that couples recognition of abortive HIV-1 RNA to induction of antiviral responses. DDX3 is ideally suited as a HIV-1 RNA sensor as it is also essential for HIV-1 replication by facilitating nuclear export[14] and translation[16,17] of HIV-1 transcripts. All HIV-1 transcripts, spliced, unspliced, abortive or full-length, share the same highly structured ~58 nt of the 5'UTR[13], and interact with DDX3. DDX3 bound to abortive HIV-1 RNAs did not assemble in translation complexes, as these abortive RNAs lack a poly(A) tail, which prevents PABP binding. Instead, the DDX3-abortive RNA complexes associated with MAVS, leading to antiviral responses. The roles of DDX3 in HIV-1 translation and antiviral defense are thus mutually exclusive, which might prevent triggering of antiviral immune responses to endogenous transcripts that also interact with DDX3[16].

Abortive HIV-1 RNAs are generated early after integration[12] and therefore DDX3-mediated type I IFN responses were induced very rapid, within 4 hours post-infection, as opposed to antiviral responses to VSV-G-pseudotyped HIV-1 that are detected 22 hours after infection of Vpx-treated DCs[35]. Abortive HIV-1 RNAs are also found in high amounts in latently infected cells[36], and it will be interesting to examine whether they can induce type I IFN responses via DDX3.

HIV-1 blocked DDX3 signaling at the level of TRAF3 recruitment to MAVS via DC-SIGN-dependent activation of PLK1. Our data underline the importance of host innate receptors for HIV-1 to suppress antiviral host defense and shows the parallel existence of various HIV-1 sensing mechanisms in DCs that are restricted in different manners[37]: while cGAS signaling after sensing of cDNA is blocked by the presence of host exonuclease TREX1[20], signaling by DDX3 after sensing of abortive transcription products was blocked by simultaneous activation

by HIV-1 via DC-SIGN of host factor PLK1. Our data also showed that viral blocking of type I IFN responses by interference at the level of MAVS was not limited to DC-SIGN signaling, as VSV-G-pseudotyped HIV-1 also inhibited MAVS signaling, even though the VSV-G envelope does not engage DC-SIGN. MAVS targeting or PLK1 activation m/ight be a versatile tool for different viruses for immune evasion. PLK1 activation can be achieved by a variety of kinases, mostly members of the broad family of Ste20-related serine/threonine kinases[29]. PLK1 activation by HIV-1_{VSV-G} might be achieved by TNF, which is induced upon infection with HIV-1_{VSV-G}, but not with HIV-1[12]. These observations also signify that the interpretation of experiments using VSV-G-pseudotyped viruses or particles should take into account the distinct effects of the VSV-G envelope.

PLK1 plays a critical role in cell division, however its role in nondividing, differentiated cells is poorly defined[38]. Our data identified PLK1 as an inhibitor of antiviral defense against HIV-1 in DCs. Although PLK1 association with MAVS blocked recruitment of TRAF3 to MAVS, the exact underlying mechanism remains to be elucidated. PLK1 could block aggregation of MAVS, which is a prerequisite for downstream signaling by MAVS to IRF3 activation[23]. Our data suggest that PLK1 inhibitors[39] could constitute a novel class of antiretroviral drugs that enhances endogenous antiviral immunity in potentially HIV-1-infected individuals.

The importance of type I IFN responses in HIV-1 infection was substantiated by the identification of two linked SNPs within the *MAVS* gene that encode a dual mutant, MAVS(Q198K-S409F), that is unable to interact with PLK1, thereby orchestrating effective antiviral defense upon HIV-1 infection via induction of DC maturation, type I IFN and proinflammatory cytokine responses. Importantly, significantly prolonged suppression of plasma viral load in HIV-1-infected individuals in a human MSM HIV-1 infection cohort was associated with homozygosity for the rare *MAVS* allele that encodes this dual mutant. The exact consequences of type I IFN responses during HIV-1 infection are a topic of debate.

Inflammation during infection is predictive of non-AIDS morbidity and death as well as high set point plasma virus load[40,41]. type I IFN responses especially are important to limit viral spread, however, during HIV-1 infection, might also create more T cell activation and therefore more HIV-1 target cells[42,43]. Inhibition of type I IFN responses in non-human primates early during SIV infection decreased expression of antiviral genes, increased SIV reservoir size and resulted in faster T cell depletion with progression to AIDS, whereas continuous exposure to type I IFN led to desensitization and increased disease progression[8]. Our data in untreated HIV-1 patients who express MAVS(Q198K-S409F) corroborate that early antiviral responses during infection are beneficial in host control of viral replication. Localized vaginal application of type I IFN shortly prior to HIV-1 exposure decreased viral replication in humanized mice[44]. Our observation that inhibition of the DDX3-MAVS blockade in primary human vaginal DCs upon HIV-1 infection restored type I IFN responses would suggest that topical therapeutic targeting would be beneficial during sexual transmission. Overall, this study underscores the importance of antiviral type I IFN responses in acute retroviral exposure, when DCs are a prominent target for HIV-1 and reveals the identified pathways as important novel targets for early therapeutic intervention to boost endogenous antiviral immunity in acute exposure or even as a prophylactic measure.

ACKNOWLEDGEMENTS

Intestinal tissue cell suspensions were kindly provided by L. Westera, C. Buskens and W. Bemelman (AMC, Amsterdam, The Netherlands). C.L. Verweij (VUmc, Amsterdam, The Netherlands) provided IFN-β, ISG15 and Mx2 primer sequences. HIV-2 virus, MT-2 cells, AZT and gp120 were obtained through the NIH AIDS Research and Reference Reagent Program. This work was supported by Aids Fonds (S.I.G.: 2012042) and the Netherlands Organisation for Scientific Research (NWO) (T.B.H.G.: VICI 918.10.619).

Author contributions. S.I.G. designed and supervised research, and performed experiments. N.H., T.M.K., E.M.Z.W., R.S.F., J.K.S., N.H.v.T., C.M.S.R. and A.A.D. performed experiments. N.H. generated 293T CRISPR KO cell lines. N.A.K. and T.B. provided ACS data. K.A.v.D. assisted with virus isolations. S.I.G. and T.B.H.G. interpreted results and wrote the paper.

FIGURE LEGENDS

- legends should be written as statements specifying experimental conditions. Use the following format: (Assay) showing (read out) in (sample) treated (treatments, conditions) for (period). Revise all legends accordingly. Please check the legends in a recently published NI article for examples.

Figure 1 Raf-1 activation suppresses type I IFN responses after HIV-1 infection of DCs. (**a-f**) Realtime PCR (RT-PCR) analyses of IFNβ (**a,c-f**) and ISG (**b**) mRNA expression in monocyte-derived (**a-c,e,f**) and primary (**d**) DCs after infection (4 h in **d-f**) with laboratory strain HIV-1_{BaL} (**a-d**), with various CCR5- and CXCR4-tropic HIV-1 strains (**e**) or with primary HIV-1 (**f**), in the absence or presence of Raf-1 inhibition (GW5074 in **a,c-f**; Raf-1 silencing (siRNA) in **b**). N.d., not determined. Mean ± SD; n = 6 (**a,c,e**), 4 (**b,f**), 2 (**d**, myeloid, vaginal, intestinal DCs) or 3 donors (**d**, dermal DCs). ** $p < 0.01$, * $p < 0.05$ (Student's *t*-test).

Figure 2 Type I IFN responses after HIV-1 infection are mediated by DDX3-MAVS. (**a-g,i,j**) RT-PCR analyses of IFNβ mRNA expression by moDCs (**a-f,j**; 4 h) or monocyte-derived macrophages (**i**; 6 h) after infection with HIV-1_{BaL}, (**a-f,i**), HIV-2_{7312A} or HTLV-1_{MT-2} (**j**) in the absence or presence of Raf inhibitor GW5074, reverse transcription inhibitor AZT or integrase inhibitor raltegravir (RAL) (**a,b**), and after silencing of TLR8 (**a**), TREX1, cGAS (**b**), DDX1, DDX5 (**c**), DDX3 (**c,d,i**) or MAVS (**e-g**). In (**d,f**), expression of DDX3 (**d**) or MAVS (**f**) was rescued by transfection with RNAi-resistant (RNAi-res) cDNAs. Mean ± SD; n = 6 (**a,c**), 3 (**b,j**), 4 (**d,f,i**) or 10 donors (**e**). ** $p < 0.01$ (Student's *t*-test). In (**h**), N_t was set at 1 for GW5074-treated HIV-1-infected moDCs (not shown). (**g**) Immunoblot (IB) analyses of immunoprecipitation (IP) of DDX3 and MAVS from untreated and GW5074-treated moDCs infected with HIV-1BAL for 3 h. β-actin served as loading control for IB analyses. Representative of 3 independent experiments. (**h**) Confocal immunofluorescence analyses of

DDX3 and mitochondria (MitoTracker) of moDCs after HIV-1 infection for 3 h. Right graphs show fluorescence intensity along marker (4 μm). Representative of 3 independent experiments.

Figure 3 DDX3 bound to capped abortive HIV-1 RNA products induces type I IFN responses via MAVS. (**a**) Immunoblot (IB) analyses of DDX3, MAVS, eIF4G, eIF4A and PABP after pulldown of m^7GTP cap-binding translation initiation complexes from moDCs 3 h after HIV-1 infection. Cap analogue m^7GpppG was used as a competitor. β-actin served as loading control. Representative of 3 independent experiments. (**b,c**) RT-PCR analyses of abortive HIV-1 RNAs and Tat-Rev HIV-1 mRNAs after RNA immunoprecipitation (IP) of DDX3, MAVS and eIF4G from moDCs treated with or without GW5074 3 h after HIV-1 infection, and after silencing of DDX3 or MAVS in moDCs (**c**). IgG and no Ab indicate negative controls. Mean ± SD; n = 3. ** $p < 0.01$, * $p < 0.05$ (Student's *t*-test). (**d-f**) RT-PCR analyses of IFNβ mRNA in moDCs 4 h after transfection with HIV-1-derived or endogenous human β-globin RNA sequences – containing either 5' m^7GTP cap (cap) and/or 3' poly(A) (poly(A)) structures or neither as indicated – after silencing of DDX3 or MAVS (**d,f**), or after crosslinking (XL) of DC-SIGN in the absence or presence of GW5074 (**e**). TAR, sequence corresponding to abortive HIV-1 RNA; Tat, sequence corresponding to full-length HIV-1 Tat transcript; β-globin, sequence corresponding to full-length human β-globin transcript. Mean ± SD; n = 8 (**d**), 4 (**e,f**). ** $p < 0.01$ (Student's *t*-test). (**g**) RT-PCR analyses of IFNβ mRNA in 293T cells depleted of either DDX3, MAVS, RIG-I and/or MDA5 expression by CRISPR-Cas9 genome editing 4 h after transfection with cap-TAR RNA coupled to LyoVec or poly(I:C)-LyoVec as a control. Mean ± SD of quadruple measurements.

Figure 4 HIV-1 infection blocks TRAF3 recruitment to MAVS and subsequent IRF3 activation. (**a,c**) RT-PCR of IFNβ mRNA by moDCs 4 h after infection with HIV-1_{BaL}, in the absence or presence of GW5074, and after silencing of TRAF3(**a**), TBK1, IKKε or IRF3 (**c**). Mean ± SD; n = 10 (**a**), 4 (**c**). ** $p < 0.01$ (Student's *t*-test). (**b**) Immunoblot (IB) analyses of DDX3, MAVS, TRAF3 and IRF3 after immunoprecipitation (IP) of DDX3 from moDCs 3 h after HIV-1 infection, with or without Raf-1 inhibition, and after silencing of MAVS, TRAF3 or TKB1/IKKε. Representative of 3 independent experiments. (**d**) Flow cytometry analyses of Ser172 phosphorylation of TBK1 and IKKε in moDCs 3 h after HIV-1 infection, with or without Raf-1 inhibition, and after silencing of DDX3 or MAVS. FI, fluorescence intensity; FSC, forward scatter. Representative of 3 independent experiments. (**e**) Immunoblot analyses of IRF3 and phosphorylated IRF3 of cytoplasmic (CE) and nuclear (NE) extracts from moDCs 3 h after HIV-1 infection, with or without GW5074, and after silencing of DDX3 or MAVS. β-actin and RNA polymerase II (RNAP2) served as loading controls. Representative of 3 independent experiments.

Figure 5 PLK1 activation during HIV-1 infection impedes TRAF3 recruitment to DDX3-MAVS and type I IFN responses. (**a,b,l**) RT-PCR analyses of IFNβ mRNA in moDCs after infection (4 h in **a,l**) with HIV-1_{BaL}, in the absence or presence of GW5074, and after silencing of PLK1 (**a,b**) or MST1 (**l**) by RNA interference. Mean ± SD; n = 6 (**a,l**), 4 (**b**). ** $p < 0.01$, * $p < 0.05$ (Student's *t*-test). (**c,d,k**) Immunoblot (IB) analyses of DDX3/MAVS and PLK1 (**c,k**) or TRAF3 (**d,k**) after immunoprecipitation of DDX3 of moDCs 3 h after HIV-1 infection, with or without GW5074 (**c**), and after silencing of MAVS (**c**), PLK1 (**d**) or MST1 (**k**). Representative of 3 independent experiments. (**e,f,j**) Immunoblot (**e**) and flow cytometry (**f,j**) analyses of Thr210 phosphorylation of PLK1 in moDCs 3 h after HIV-1 infection or gp120 stimulation (**f**), with or without Raf-1 (**e,f**) or DC-SIGN (**f**) inhibition, and

after silencing of MST1 (**j**). β-actin served as loading control (**e**). Representative of 2 (**e**), 6 (**f**, HIV-1), 4 (**f**, gp120), 5 (**j**) independent experiments. (**g**) ELISA of Thr210 phosphorylation of Flag-PLK1 by recombinant kinases. (**h,i**) Kinase activity assay or of MST1 activity (**h**) or flow cytometry analyses of Thr183 autophosphorylation (**i**) in moDCs after HIV-1 infection or gp120 stimulation (1 h in **i**), with or without Raf-1 (**h,i**) and DC-SIGN (**h**) inhibition. Mean ± SD; n = 4 (**h**). Representative of 2 (**i**) independent experiments. ** $p < 0.01$, * $p < 0.05$ (Student's *t*-test).

Figure 6 IFN-I responses by DCs suppress HIV-1 replication in infected individuals. (**a, d**) Flow cytometry analyses of HIV-1 p24 expression in DCs (% $p24^+$) at 3, 5 and 7 days post-infection, with or without IFNR inhibition, and after PLK1 silencing (**a**) or in moDCs expressing either wild-type MAVS (homozygous for major alleles of rs7262903/rs7269320) or dual MAVS K198/F409 mutant (homozygous for minor alleles) (**d**). Mean ± SD of duplicates; representative of 4 (**a**), 5 (**d**, Major), 3 (**d**, Minor) independent experiments. (**b**) HIV-1 RNA levels (log_{10} viral copies/ml plasma) at set point in untreated HIV-1-infected individuals in a human MSM cohort, differentiated based on genotype of linked *MAVS* SNPs rs7262903/rs7269320 (Minor, homozygous for minor alleles; Hz, heterozygous for both alleles; Major, homozygous for major alleles). *P* values calculated using unpaired Student's *t*-test. (**c**) Kaplan-Meier survival curve comparing the time required for log_{10} viral copies/ml plasma to reach >4.5 (VL, viral load) from seroconversion (SC), in untreated HIV-1-infected individuals in a human MSM cohort, differentiated on genotype as in (**b**). *P* value calculated using Cox regression model.

Figure 7 PLK1-mediated suppression of DDX3 signaling after HIV-1 infection is impeded by mutation of MAVS. (**a,k**) RT-PCR analyses of IFNβ mRNA by moDCs with

either major or minor genotype for *MAVS* SNPs rs7262903/rs7269320 6 h after transfection with poly(I-C)-LyoVec, 24 h after infection with rMV^{KS} (**a**) or 4 h after infection with HIV-1_{VSV-G}, after silencing of DDX3 (**k**). Mean ± SD; n = 3 (**a**), 2 (**k**). (**b-e,g**) RT-PCR analyses of IFNβ (**b,d,e,g**) and ISG (**c**) mRNA in moDCs (dermal DCs in **d**) with either heterozygous (Hz) or minor rs7262903/rs7269320 genotypes, after infection (4 h in **d,e,g**) with HIV-1_{BaL}, in the absence or presence of Raf inhibitor GW5074, and after silencing of DDX3, MAVS (**e**) or PLK1 (**g**). Mean ± SD; n = 4 (**b**, Hz), 3 (**b**, Minor; **c**;**d**, Hz; **e**;**g**), 2 (**d**, Minor; **k**). ** $p < 0.01$ (Student's *t*-test). (**f**) Immunoblot (IB) analyses of immunoprecipitation (IP) of DDX3 for DDX3/MAVS, TRAF3 and PLK1 from moDCs with minor rs7262903/rs7269320 genotype 3 h after HIV-1 infection, with or without Raf-1 inhibition. β-actin served as loading control. Representative of 3 independent experiments. (**h**) Flow cytometry analyses of Thr210 phosphorylation of PLK1 in moDCs with minor rs7262903/rs7269320 genotype 3 h after HIV-1 infection, with or without Raf-1 or DC-SIGN inhibition. Representative of 3 independent experiments. (**i**) ELISA of association between Thr210-phosphorylated Flag-PLK1 and wild-type MAVS (moDC lysate major genotype) or dual MAVS K198/F409 mutant (moDC lysate minor genotype). Mean ± SD; n = 3. * $p < 0.05$ (unpaired Student's *t*-test). (**j**) RT-PCR analyses of IFNβ mRNA in MAVS-silenced moDCs 4 h after infection with HIV-1_{BaL}, in the absence or presence of Raf inhibitor GW5074, after complementation of MAVS expression by transfection with RNAi-resistant cDNAs encoding single (QF, Q198/F409; KS, K198/S409) or dual (KF, K198/F409) MAVS mutants. Mean ± SD; n = 4. ** $p < 0.01$ (Student's *t*-test).

Figure 8 HIV-1 infection attenuates DDX3/MAVS-mediated DC maturation and IL-1β expression. (**a-c**) Flow cytometry analyses of expression of maturation markers CD80, CD83 and CD86 on DCs with either major (**a,b**) or minor (**c**) rs7262903/rs7269320 genotypes, 48 h

after infection with HIV-1_{BaL}, in the absence or presence of Raf inhibitor GW5074, with or without IFNR inhibition (**a,c**), and after silencing of DDX3, MAVS or PLK1 (**b**). FI, fluorescence intensity. Representative of 5 (**a**), 6 (**b**) and 3 (**c**) independent experiments. (**d-h**) RT-PCR analyses and ELISA of IL-1β mRNA (**d,f-h**) and protein (**e**) expression, respectively, by DCs with either major (**d-g**), heterozygous (Hz) or minor (**h**) rs7262903/rs7269320 genotypes, after HIV-1 infection (48 h in **E**; 10 h in **F, G**), with or without Raf-1 inhibition, with or without IFNR inhibition (**G**), and after silencing of DDX3, MAVS or PLK1 (**f**). Mean ± SD; n = 6 (**d**), 4 (**e**;**f**; **h**, Hz), 5 (**g**), 2 (**h**, Minor). ** $p < 0.01$, * $p < 0.05$ (Student's *t*-test).

METHODS

DC and macrophage isolation. Monocyte-derived DCs were generated from blood of healthy volunteer donors (Sanquin) as described[45]. Monocyte-derived macrophages were generated from isolated monocytes by culturing in RPMI medium with 10% FCS and 50 ng/ml M-CSF (Immunotools) for 7 days, while 500 U/ml IL-4 (Invitrogen) was added for the last 48 h. Primary DCs were isolated from blood of healthy volunteer donors, skin and vaginal tissues obtained from healthy individuals undergoing reconstructive plastic procedure or vaginal prolapse surgery, respectively, and healthy bowel tissues from cancer or colitis ulcerosa patients undergoing colectomy. Tissue harvesting procedures were approved by the AMC Medical Ethics Committee. Split-skin grafts 0.3 mm in thickness were obtained using a dermatome (Zimmer) and digested for 45 min at 37°C with 2 μg/ml dispase II (Roche Diagnostics) to separate dermis from epidermis. Dermis and vaginal tissues were further treated with 5 mg/ml collagenase D and 200 U/ml DNase I (both Roche diagnostics) for 90 min at 37°C after mechanic fragmentation using forceps and scissors. Mucosa from bowel tissues was separated from underlying tissues using scissors, digested with 1 mg/ml collagenase D, 50 μg/ml DNase I (both Roche diagnostics) and 1 mg/ml soybean trypsin inhibitor (Invitrogen) for 1 h at 37°C, followed by mechanical dissociation using the GentleMACS Dissociator (Myltenyi). Digested tissues were then passed over a 100 μM cell strainer (Greiner) to obtain single cell suspensions. DC-SIGN$^+$ cells were then isolated using CD209 MicroBead kit (Miltenyi Biotec). Blood and tissues were routinely screened for SNPs rs7262903, rs7269320, and rs7267297 using TaqMan genotyping Assays (ID C_25623847, C_25623845, and C_29168352; Applied Biosystems); only cells with the major genotype profile for all three SNPs were used, unless otherwise stated.

293T CRISPR/Cas9 KO cell lines. 293T cells were transfected with 2 μg CRISPR/Cas9 KO plasmids (control, sc-418922; DDX3, sc-419975; MAVS, sc-400769; RIG-I, sc-432915; MDA5, sc-401962; all Santa Cruz) using GeneJuice transfection reagent (Novagen) as described by the manufacturer. The KO plasmids are a mixture of 3 plasmids each carrying a different guide RNA to the target gene as well as the Cas and GFP coding regions. GFP^+ cells were selected by sorting on a SH800S Cell Sorter (Sony Biotechnology) 24 to 48 h after transfection, and depletion of target proteins was verified by immunoblotting (**Supplementary Fig. 4**).

Cell treatment. Cells were stimulated with 10 ng/ml LPS from *Salmonella typhosa* (Sigma), 5 μg/ml R848, 10 μg/ml MDP, 1 μg/ml poly(I:C)-LyoVec, 1 μg/ml 3'3'-cGAMP, 1 μg/ml HSV DNA-LyoVec (all Invivogen), 10 μg/ml recombinant gp120 (NIH AIDS Research and Reference Reagent Program), or 10 μM RNA sequences corresponding to either abortive HIV-1 RNA, full-length HIV-1 Tat transcripts or full length human β-globin transcripts coupled to LyoVec (Invivogen) as described by the manufacturer. The RNA sequences were produced via *in vitro* transcription (IVT) by BioSynthesis (www.biosyn.com); 5' m^7GTP structures were added during IVT by co-capping, while 3' poly(A) was added by enzymatic tailing. DC-SIGN crosslinking with antibodies was performed as described[45]. Sequences are listed in **Supplementary Table 1**. Cells were infected with HIV-1, HIV-2, HTLV-1 and HIV-1_{VSV-G} at MOI 0.1-0.4 (see below) or rMS^{KV} (see ref [45]) as described. Preincubation with inhibitors or blocking antibodies was done for 2 h: 1 μM GW5074 (Calbiochem), 5 μg/ml AZT (NIH AIDS Research and Reference Reagent Program), 50 nM Raltegravir (Merck), 20 μg/ml anti-DC-SIGN (AZN-D1), 20 μg/ml anti-IFNα/βR2 (MMHAR-2; PBL Interferon Source) and 20 μg/ml mouse IgG2a isotype (14-4724-85; eBioscience) as control. DCs were transfected with 25 nM siRNA using transfection reagent DF4 (Dharmacon) and used for

experiments 72 h later. SMARTpool siRNAs used were: Raf-1 (M-003601-02), TLR8 (M-004715-01), TREX1 (M-013239-03), cGAS (M-015607-01), STING (M-024333-00), RIG-I (M-012511-01), MDA5 (M-013041-00), DDX1 (M-011993-00), DDX3 (M-006874-01), DDX5 (M-003774-01), MAVS (M-024237-02), TRAF3 (M-005252-02), TBK1 (M-003788-02), IKKε (M-003723-02), IRF3 (M-006875-02), PLK1 (M-003290-01) and non-targeting siRNA (D-001206-13) as a control; ON-TARGET plus siRNA used was: MST1 (L-008946-02) (all Dharmacon). Silencing of expression was verified by real-time PCR, flow cytometry and immunoblotting (**Supplementary Fig. 8** and **Supplementary Table 2**); antibodies used flow verification were: anti-Raf-1 (9422; Cell Signaling), anti-TLR8 (sc-25467; Santa Cruz), anti-RIG-I (3743; Cell Signaling), anti-MDA5 (4109; Cell Signaling), anti-TREX1 (12215; Cell Signaling), anti-cGAS (15102; Cell Signaling), anti-STING (13647; Cell Signaling), anti-DDX1 (ab151962, Abcam), anti-DDX3 (2635; Cell Signaling), anti-DDX5 (ab128928, Abcam), anti-MAVS (3993; Cell Signaling), anti-TRAF3 (4729; Cell Signaling), anti-TBK1 (3504; Cell Signaling), anti-IKKε (2905; Cell Signaling), anti-IRF3 (sc-9082; Santa Cruz), anti-PLK1 (4513; Cell Signaling) and anti-MST1 (ab57836, Abcam), followed by incubation with either PE-conjugated anti-rabbit (711-116-152; Jackson Immunoresearch) or Alexa488-conjugated anti-mouse (A11029; Invitrogen) (flow cytometry), or with HRP-conjugated secondary antibody (21230; Pierce) or anti-mouse (sc-2314; Santa Cruz) followed by ECL detection (Pierce) (immunoblotting). Rescue of DDX3 or MAVS expression after silencing was achieved by transfecting DCs for 48 h with LyoVec-coupled (see above) pcDNA3-based expression plasmids containing cDNAs with synonymous mutations that rendered them resistant to the used DDX3 and MAVS siRNAs. MAVS cDNA was further modified to encode single Q198K or S409F and dual Q198K/S409F mutants. Plasmids were generated by Life Technologies (ThermoFisher Scientific). Expression of transfected DDX3 and MAVS

was verified by flow cytometry using anti-DDX3 (2635; Cell Signaling) and anti-MAVS (3993; Cell Signaling) (**Supplementary Fig. 7**).

MSM cohort. Untreated HIV-1-infected MSM participating in the Amsterdam cohort studies (ACS) on HIV-1 infection and AIDS (http://www.amsterdamcohortstudies.org) were genotyped and used for subsequent analyses. Treatment details and exclusion criteria have been described[46]. ACS are conducted in accordance with ethical principles set out in the declaration of Helsinki and approved by the AMC Medical Ethics Committee; all participants provided written informed consent.

Viruses and infection. HIV-1_{BaL}, HIV-1_{SF162}, HIV-1_{R9} and HIV-1_{LAI} as well as VSV-G-pseudotyped HIV-1 NL4.3-Δenv were produced and titers quantified as described[12,47]. Clinical HIV-1 isolates were produced as described[48]. HIV-2 7312A was obtained through the NIH AIDS Research and Reference Reagent Program. HTLV-1 virus was isolated from supernatant of MT-2 cells (NIH AIDS Research and Reference Reagent Program). DCs or macrophages were infected at MOI 0.1-0.4; infection was determined by viral transcript (Tat-Rev, Tax-Rex[49], Vpu) quantification or flow cytometry (p24). mRNA isolation, cDNA synthesis and real-time PCR were performed as described[12]; relative mRNA expression was obtained by setting N_t ($=2^{Ct(GAPDH)-Ct(target)}$) at 1 in 4 h (Tat-Rev, Tax-Rex) or 10 h (Vpu) HIV-1-infected DCs, within one experiment and for each donor, except time course experiments where $N_t = 1$ at 8 h (Tat-Rev). Primers are listed in **Supplementary Table 2**. Intracellular p24 was detected after 3, 5 and 7 days by anti-p24 (KC57-RD1; Beckman Coulter).

Immune responses. IFNβ, ISG and IL-1β mRNA were quantified as above; N_t was set at 1 in 4 h (IFNβ), 8 h (ISGs) or 10 h (IL-1β) GW5074-treated HIV-1-infected DCs. Primers are

listed in **Supplementary Table 2**. IL-1β in supernatants was measured 48 h post-infection by ELISA (Invitrogen). DC maturation was determined 48 h post-infection by flow cytometry analysis of CD80 (557227; BD), CD83 (555658; BD) and CD86 (PN1M2218; Beckmann Coulter) cell surface expression.

Association of DDX3-MAVS-TRAF3-IRF3 and PLK1. Whole cell extracts of HIV-1-infected DCs were prepared 3 h post-infection using RIPA Buffer (Cell Signaling). DDX3- or MAVS-associated proteins were immunoprecipitated from 40 μg of extract with 4 μg anti-DDX3 (sc-98711) or anti-MAVS (sc-68926; both Santa Cruz) coated on protein A/G-PLUS agarose beads (Santa Cruz). Either 20 μg of extract or immunoprecipitates were resolved by SDS-PAGE, and detected by immunoblotting with anti-DDX3 (2635; Cell Signaling), anti-MAVS (3993; Cell Signaling), anti-TRAF3 (4729; Cell Signaling), anti-IRF3 (sc-9082; Santa Cruz) or anti-PLK1 (4513; Cell Signaling), followed by incubation with HRP-conjugated secondary antibody (21230; Pierce) and ECL detection (Pierce). To ensure equal protein content prior to immunoprecipitation, membranes were also incubated with anti-β-actin (sc-81178; Santa Cruz), followed by HRP-conjugated anti-mouse (sc-2314; Santa Cruz).

Association of DDX3 with mitochondrial MAVS was visualized by confocal microscopy. DCs were infected for 3 h, while during the last 30 min 200 nM MitoTracker Red CMXRos (Cell Signaling) was added to the medium. Cells were then fixed with 4% *para*-formaldehyde, permeabilized with 0.2% (vol/vol) Triton X-100 in PBS, and stained with anti-DDX3 (sc-98711; Santa Cruz) together with 1 μg/ml Hoechst (Invitrogen). Visualization was done with a Leica TCS SP8 X confocal microscope.

Association of PLK1 with either wild-type or mutant MAVS was further examined by capture ELISA. 50 ng Thr210-phosphorylated Flag-PLK1 (Origene; see below) was immobilized on anti-PLK1 (4513; Cell Signaling)-coated high-binding 96-wells plates and incubated with

whole cell extracts (see above) of immature DCs from donors with either the minor or major genotype for rs7262903/rs7269320. MAVS associated with PLK1 was detected with anti-MAVS (3993; Cell Signaling), followed by incubation with HRP-conjugated anti-rabbit IgG (7074; Cell Signaling) and assayed using TMB substrate. After termination of the coloring reaction, the absorbance was measured at 450 nm.

Activation of TBK1, IKKε, IRF3, PLK1, and MST1. Phosphorylation of TBK1, IKKε, PLK1, and MST1 in HIV-1-infected DCs was detected 1 h (MST1) or 3 h (TBK1, IKKε, PLK1) post-infection by flow cytometry. Cells were first fixed in 3% *para*-formaldehyde for 10 min and permeabilized in 90% methanol at 4°C for 30 min. Primary antibody incubation with anti-TBK1 p-S172 (5483; Cell Signaling), anti-IKKε p-S172 (06-1340; Millipore), anti-PLK1 p-T210 (5472; Cell Signaling) or MST1 p-T183 (3681; Cell Signaling) was followed by incubation with PE-conjugated anti-rabbit (711-116-152; Jackson Immunoresearch). Phosphorylation was analyzed on a FACS Calibur (BD).

Phosphorylated PLK1 was also detected by immunoblotting. 40 μg of whole cell extracts (see above) were resolved by SDS-PAGE, and detected by immunoblotting with anti-PLK1 (4513; Cell Signaling) or anti-PLK1 p-T210 (5472; Cell Signaling), followed by incubation with HRP-conjugated secondary antibody (21230; Pierce) and ECL detection (Pierce). To ensure equal protein content prior to immunoprecipitation, membranes were also incubated with anti-β-actin (sc-81178; Santa Cruz), followed by HRP-conjugated anti-mouse (sc-2314; Santa Cruz).

Flag-PLK1 (Origene) was captured on anti-FLAG (F1804; Sigma)-coated high-binding 96-wells plates and treated with 100 ng/ml recombinant active kinase (Raf-1, Millipore; MST1, Promega; PKA, Active Motif) in kinase activity buffer (50 mM Tris-HCl [pH 7.5], 10 mM $MgCl_2$, 50 μM DTT, 50 μM ATP, 25 mM β-glycerophosphate, 0.006% Brij-35) for 30 min at

30°C. Thr210 phosphorylation was then detected with anti-PLK1 p-T210 (5472; Cell Signaling), followed by incubation with HRP-conjugated anti-rabbit IgG (7074; Cell Signaling) and assayed using TMB substrate. Equal capture of Flag-PLK1 was determined with anti-PLK1 (4513; Cell Signaling).

Nuclear translocation of IRF3 was determined in cytoplasmic (CE) and nuclear extracts (NE) of HIV-1-infected DCs prepared 3 h post-infection using NucBuster protein extraction kit (Novagen). 10 μg CE and 20 μg NE were resolved by SDS-PAGE, and IRF3 was detected by immunoblotting with anti-IRF3 (sc-9082; Santa Cruz) and anti-IRF3 p-S396 (29047; Cell Signaling), followed by incubation with HRP-conjugated secondary antibody (21230; Pierce) and ECL detection (Pierce). Membranes were also probed with anti-RNAPII (clone CTD4H8; Millipore) or anti-β-actin (sc-81178; Santa Cruz), followed by HRP-conjugated anti-mouse (sc-2314; Santa Cruz) to ensure equal protein loading among CE and NE, respectively.

MST1 kinase activity was measured using MST1 kinase enzyme system in combination with ADP-Glo kinase assay (both Promega). Kinase whole cell extracts were prepared at indicated times using MST1 lysis buffer (25 mM Tris-HCl [pH 7.5], 25 mM $MgCl_2$, 2 mM EDTA, 250 μM DTT, 12.5 mM β-glycerophosphate, 1% Triton X-100, 10 μg/ml leupeptin, 10 μg/ml pepstatin A, 0.4 mM PMSF). MST1 was captured from 10 μg of extract in anti-MST1 (ab57836; Abcam)-coated high-binding 96-wells plates. 5 μg substrate (Axltide) was added in 20 μl kinase activity buffer (see above) and incubated for 45 min at 30°C. Generated ADP was then measured using ADP-Glo kinase assay; the detected relative light units (RLU) are a measure for MST1 activity.

Translation initiation complex composition. Cytoplasmic extracts of HIV-1-infected DCs prepared 3 h post-infection using ChIP lysis buffer (Active Motif) were treated with micrococcal nuclease (Cell Signaling) for 30 min at 37°C. Translation initiation complexes

were retained on m^7GTP-agarose (Jena Bioscience) from 40 ug of nuclease-treated extracts, with cap analogue m^7GpppG (New England Biolabs) as competitor as described[17], resolved by SDS-PAGE, and detected by immunoblotting with anti-DDX3 (2635; Cell Signaling), anti-MAVS (3993; Cell Signaling), anti-eIF4G (2498; Cell Signaling), anti-eIF4A (2425; Cell Signaling) or anti-PABP (4992; Cell Signaling), followed by incubation with HRP-conjugated secondary antibody (21230; Pierce) and ECL detection (Pierce). To ensure equal protein content prior to m^7GTP cap binding, membranes were also incubated with anti-β-actin (sc-81178; Santa Cruz), followed by HRP-conjugated anti-mouse (sc-2314; Santa Cruz).

RNA immunoprecipitation (RIP) assay. RIP and re-RIP assays were performed using EZ-MagnaRIP kit (Millipore). Briefly, DCs were fixed with 1% (vol/vol) *para*-formaldehyde and lysed. Protein-RNA complexes were immunoprecipitated from the equivalent of 1 million cells using 2 μg anti-DDX3 (sc-98711; Santa Cruz), anti-MAVS (sc-68926; Santa Cruz), anti-eIF4G (2498; Cell Signaling), or negative control IgG (sc-2027; Santa Cruz), and protein G-coated magnetic beads. For re-RIP analyses, DDX3-RNA complexes were eluted from beads, desalted, and a second round of immunoprecipitation was performed with anti-MAVS or anti-eIF4G. RNA-protein crosslinks were reversed in 200 mM NaCl for 2 h at 70°C, before proteinase K treatment for 1 h at 37°C. mRNA and non-mRNA fractions were separated, isolated and quantified as described, using strict controls to ensure that abortive HIV-1 RNA is measured in non-mRNA samples without cross-contamination with either genomic DNA or mRNA[12]. Primers are listed in **Supplementary Table 1**. To normalize for RNA input, a sample for each condition was taken along which had not undergone immunoprecipitation; results are expressed as % input RNA.

Statistical analysis. Used methods are Student's *t*-test for paired (mRNA, MST1) or unpaired (set point plasma viral load, MAVS-PLK1 ELISA) observations. Cox regression model was used for time-to-event outcomes, without controlling for multiple testing. Statistical significance was set at $p < 0.05$.

Data availability

The data that support the findings of this study are available from the corresponding author upon reasonable request.

REFERENCES

1. Steinman, R.M. Decisions about dendritic cells: past, present, and future. *Annu. Rev. Immunol.* **30**, 1-22 (2012).

2. Miller, E. & Bhardwaj, N. Dendritic cell dysregulation during HIV-1 infection. *Immunol. Rev.* **254**, 170-189 (2013).

3. Goujon, C. *et al.* Human MX2 is an interferon-induced post-entry inhibitor of HIV-1 infection. *Nature* **502**, 559-562 (2013).

4. Kane, M. *et al.* MX2 is an interferon-induced inhibitor of HIV-1 infection. *Nature* **502**, 563-566 (2013).

5. Yan, N. & Chen, Z.J. Intrinsic antiviral immunity. *Nat. Immunol.* **13**, 214-222 (2012).

6. Simmons, D.P. *et al.* Type I IFN drives a distinctive dendritic cell maturation phenotype that allows continued class II MHC synthesis and antigen processing. *J. Immunol.* **188**, 3116-3126 (2012).

7. González-Navajas, J.M., Lee, J., David, M. & Raz, E. Immunomodulatory functions of type I interferons. *Nat. Rev. Immunol.* **12**, 125-135 (2012).

8. Sandler, N.G. *et al.* Type I interferon responses in rhesus macaques prevent SIV infection and slow disease progression. *Nature* **511**, 601-605 (2014).

9. Gringhuis, S.I. *et al.* C-type lectin DC-SIGN modulates Toll-like receptor signaling via Raf-1 kinase-dependent acetylation of transcription factor NF-kappaB. *Immunity* **26**, 605-616 (2007).

10. Gringhuis, S.I., den Dunnen, J., Litjens, M., van der Vlist, M. & Geijtenbeek, T.B.H. Carbohydrate-specific signaling through the DC-SIGN signalosome tailors immunity to Mycobacterium tuberculosis, HIV-1 and Helicobacter pylori. *Nat. Immunol.* **10**, 1081-1088 (2009).

11. Solis, M. *et al.* RIG-I-mediated antiviral signaling is inhibited in HIV-1 infection by a protease-mediated sequestration of RIG-I. *J. Virol.* **85**, 1224-1236 (2011).

12. Gringhuis, S.I. *et al.* HIV-1 exploits innate signaling by TLR8 and DC-SIGN for productive infection of dendritic cells. *Nat. Immunol.* **11**, 419-426 (2010).

13. Kao, S.Y., Calman, A.F., Luciw, P.A. & Peterlin, B.M. Anti-termination of transcription within the long terminal repeat of HIV-1 by tat gene product. *Nature* **330**, 489-493 (1987).

14. Yedavalli, V.S., Neuveut, C., Chi, Y.H., Kleiman, L. & Jeang, K.T. Requirement of DDX3 DEAD box RNA helicase for HIV-1 Rev-RRE export function. *Cell* **119**, 381-392 (2004).

15. Naji, S. *et al.* Host cell interactome of HIV-1 Rev includes RNA helicases involved in multiple facets of virus production. *Mol. Cell. Proteomics* **11**, M111 (2012).

16. Soto-Rifo, R. *et al.* DEAD-box protein DDX3 associates with eIF4F to promote translation of selected mRNAs. *EMBO J.* **31**, 3745-3756 (2012).

17. Soto-Rifo, R., Rubilar, P.S. & Ohlmann, T. The DEAD-box helicase DDX3 substitutes for the cap-binding protein eIF4E to promote compartmentalized translation initiation of the HIV-1 genomic RNA. *Nucleic Acids Res.* **41**, 6286-6299 (2013).

18. Goubau, D., Deddouche, S. & Reis e Sousa Cytosolic sensing of viruses. *Immunity* **38**, 855-869 (2013).

19. Gao, D. *et al.* Cyclic GMP-AMP synthase is an innate immune sensor of HIV and other retroviruses. *Science* **341**, 903-906 (2013).

20. Yan, N., Regalado-Magdos, A.D., Stiggelbout, B., Lee-Kirsch, M.A. & Lieberman, J. The cytosolic exonuclease TREX1 inhibits the innate immune response to human immunodeficiency virus type 1. *Nat. Immunol.* **11**, 1005-1013 (2010).

21. Lahouassa, H. *et al.* SAMHD1 restricts the replication of human immunodeficiency virus type 1 by depleting the intracellular pool of deoxynucleoside triphosphates. *Nat Immunol* **13**, 223-228 (2012).

22. Hertoghs, N. *et al.* SAMHD1 degradation enhances active suppression of dendritic cell maturation by HIV-1. *J. Immunol.* in press (2015).

23. Hou, F. *et al.* MAVS forms functional prion-like aggregates to activate and propagate antiviral innate immune response. *Cell* **146**, 448-461 (2011).

24. Clark, K., Plater, L., Peggie, M. & Cohen, P. Use of the pharmacological inhibitor BX795 to study the regulation and physiological roles of TBK1 and IkappaB kinase epsilon: a distinct upstream kinase mediates Ser-172 phosphorylation and activation. *J. Biol. Chem.* **284**, 14136-14146 (2009).

25. Liu, S. *et al.* Phosphorylation of innate immune adaptor proteins MAVS, STING, and TRIF induces IRF3 activation. *Science* **347**, aaa2630 (2015).

26. Saha, S.K. *et al.* Regulation of antiviral responses by a direct and specific interaction between TRAF3 and Cardif. *EMBO J.* **25**, 3257-3263 (2006).

27. Vitour, D. *et al.* Polo-like kinase 1 (PLK1) regulates interferon (IFN) induction by MAVS. *J. Biol. Chem.* **284**, 21797-21809 (2009).

28. Elia, A.E. *et al.* The molecular basis for phosphodependent substrate targeting and regulation of Plks by the Polo-box domain. *Cell* **115**, 83-95 (2003).

29. Ji, J.H. *et al.* Purification and proteomic identification of putative upstream regulators of polo-like kinase-1 from mitotic cell extracts. *FEBS Lett.* **584**, 4299-4305 (2010).

30. Rabizadeh, S. *et al.* The scaffold protein CNK1 interacts with the tumor suppressor RASSF1A and augments RASSF1A-induced cell death. *J. Biol. Chem.* **279**, 29247-29254 (2004).

31. Praskova, M., Khoklatchev, A., Ortiz-Vega, S. & Avruch, J. Regulation of the MST1 kinase by autophosphorylation, by the growth inhibitory proteins, RASSF1 and NORE1, and by Ras. *Biochem J.* **381**, 453-462 (2004).

32. de Roda Husman, A.M. *et al.* Association between CCR5 genotype and the clinical course of HIV-1 infection. *Ann. Intern. Med.* **127**, 882-890 (1997).

33. Pothlichet, J. *et al.* A loss-of-function variant of the antiviral molecule MAVS is associated with a subset of systemic lupus patients. *EMBO Mol. Med.* **3**, 142-152 (2011).

34. Pertel, T., Reinhard, C. & Luban, J. Vpx rescues HIV-1 transduction of dendritic cells from the antiviral state established by type 1 interferon. *Retrovirology.* **8**, 49 (2011).

35. Manel, N. *et al.* A cryptic sensor for HIV-1 activates antiviral innate immunity in dendritic cells. *Nature* **467**, 214-217 (2010).

36. Adams, M. *et al.* Cellular latency in human immunodeficiency virus-infected individuals with high CD4 levels can be detected by the presence of promoter-proximal transcripts. *Proc. Natl. Acad. Sci. U. S. A* **91**, 3862-3866 (1994).

37. Luban, J. Innate immune sensing of HIV-1 by dendritic cells. *Cell Host Microbe* **12**, 408-418 (2012).

38. Archambault, V. & Glover, D.M. Polo-like kinases: conservation and divergence in their functions and regulation. *Nat. Rev. Mol. Cell. Biol.* **10**, 265-275 (2009).

39. Li, S., Zhang, Y. & Xu, W. Developments of polo-like kinase 1 (Plk1) inhibitors as anti-cancer agents. *Mini. Rev. Med. Chem.* **13**, 2014-2025 (2013).

40. Hunt, P.W. *et al.* Gut epithelial barrier dysfunction and innate immune activation predict mortality in treated HIV infection. *J. Infect. Dis.* **210**, 1228-1238 (2014).

41. Roberts, L. *et al.* Genital tract inflammation during early HIV-1 infection predicts higher plasma viral load set point in women. *J. Infect. Dis.* **205**, 194-203 (2012).

42. Fernandez, S. *et al.* CD4+ T-cell deficiency in HIV patients responding to antiretroviral therapy is associated with increased expression of interferon-stimulated genes in CD4+ T cells. *J. Infect. Dis.* **204**, 1927-1935 (2011).

43. Fraietta, J.A. *et al.* Type I interferon upregulates Bak and contributes to T cell loss during human immunodeficiency virus (HIV) infection. *PLoS Pathog.* **9**, e1003658 (2013).

44. Wheeler, L.A. *et al.* TREX1 knockdown induces an interferon response to HIV that delays viral infection in humanized mice. *Cell Rep.* **15**, 1715-1727 (2016).

45. Mesman, A.W. *et al.* Measles virus suppresses RIG-I-like receptor activation in dendritic cells via DC-SIGN-mediated inhibition of PP1 phosphatases. *Cell Host Microbe* **16**, 31-42 (2014).

46. Booiman, T., Setiawan, L.C. & Kootstra, N.A. Genetic variation in Trex1 affects HIV-1 disease progression. *AIDS* **28**, 2517-2521 (2014).

47. Sarrami-Forooshani, R. *et al.* Human immature Langerhans cells restrict CXCR4-using HIV-1 transmission. *Retrovirology* **11**, 52 (2014).

48. Quakkelaar, E.D. *et al.* Susceptibility of recently transmitted subtype B human immunodeficiency virus type 1 variants to broadly neutralizing antibodies. *J. Virol.* **81**, 8533-8542 (2007).

49. Kinoshita, T. *et al.* Detection of mRNA for the tax1/rex1 gene of human T-cell leukemia virus type I in fresh peripheral blood mononuclear cells of adult T-cell leukemia patients and viral carriers by using the polymerase chain reaction. *Proc. Natl. Acad. Sci. U. S. A.* **86**, 5620-5624 (1989).

FIgure 1.

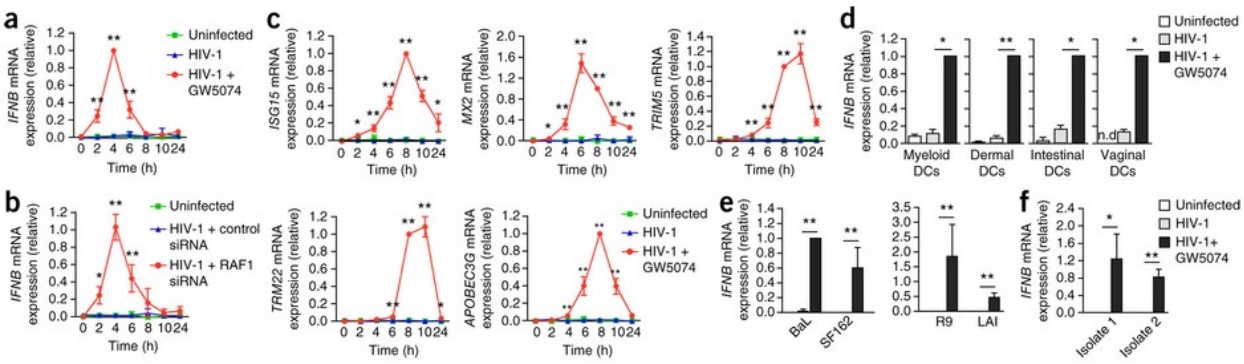
a
IFNB mRNA expression (relative)
Time (h)
Uninfected
HIV-1
HIV-1 + GW5074
b
HIV-1 + control siRNA
HIV-1 + RAF1 siRNA
c
ISG15 mRNA expression (relative)
MX2 mRNA expression (relative)
TRIM5 mRNA expression (relative)
TRM22 mRNA expression (relative)
APOBEC3G mRNA expression (relative)
d
Myeloid DCs
Dermal DCs
Intestinal DCs
Vaginal DCs
n.d
e
BaL
SF162
R9
LAI
f
Isolate 1
Isolate 2
HIV-1+ GW5074

Figure 2

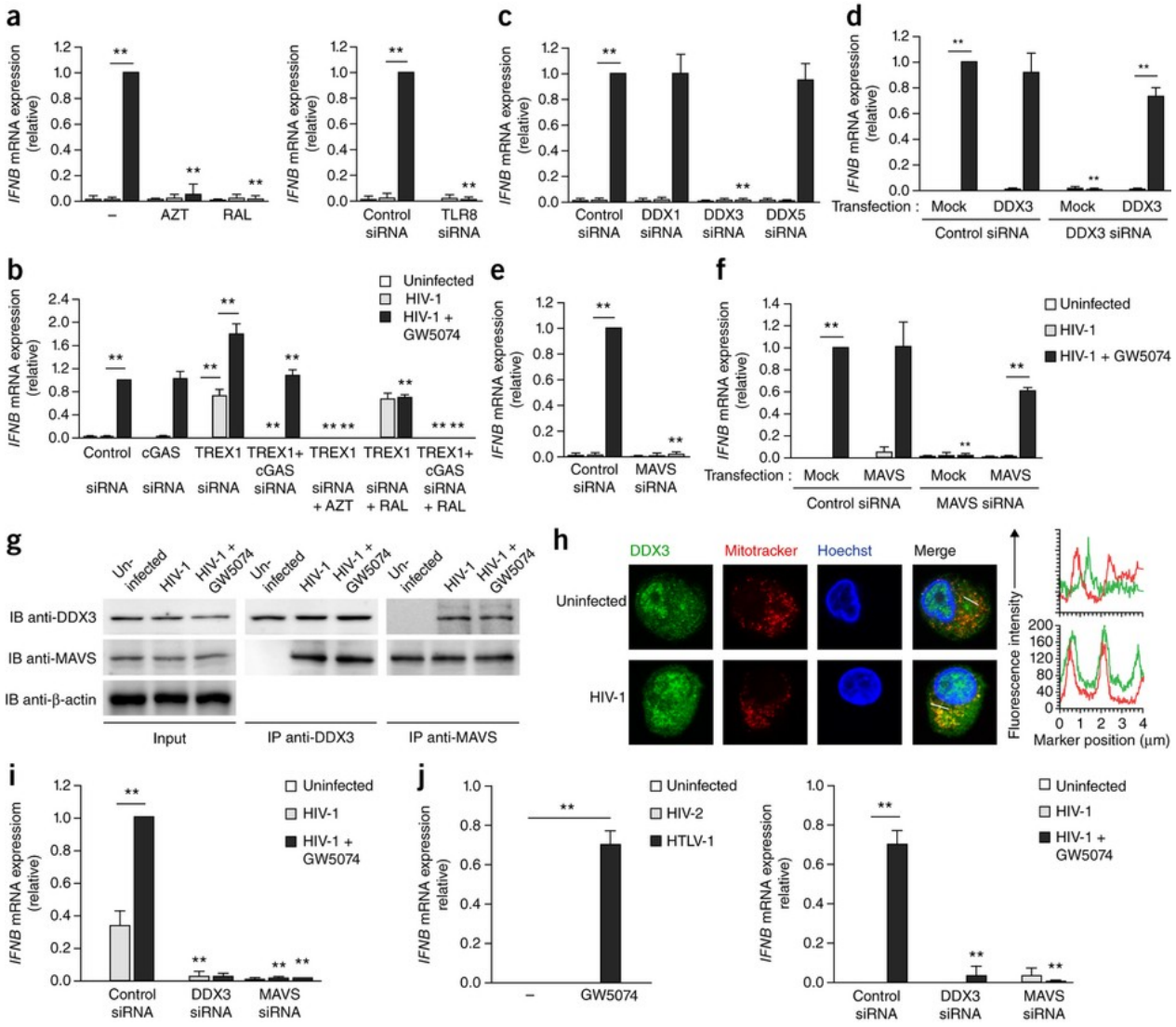
a
IFNB mRNA expression (relative)
–
AZT
RAL
Control siRNA
TLR8 siRNA
c
Control siRNA
DDX1 siRNA
DDX3 siRNA
DDX5 siRNA
d
Transfection :
Mock
DDX3
Control siRNA
DDX3 siRNA
b
Uninfected
HIV-1
HIV-1 + GW5074
Control siRNA
cGAS siRNA
TREX1 siRNA
TREX1+ cGAS siRNA
TREX1 siRNA + AZT
TREX1 siRNA + RAL
TREX1+ cGAS siRNA + RAL
e
MAVS siRNA
f
g
Un-infected
HIV-1
HIV-1 + GW5074
IB anti-DDX3
IB anti-MAVS
IB anti-β-actin
Input
IP anti-DDX3
IP anti-MAVS
h
DDX3
Mitotracker
Hoechst
Merge
Uninfected
HIV-1
Fluorescence intensity
Marker position (μm)
i
j
HIV-2
HTLV-1
GW5074

Figure 3

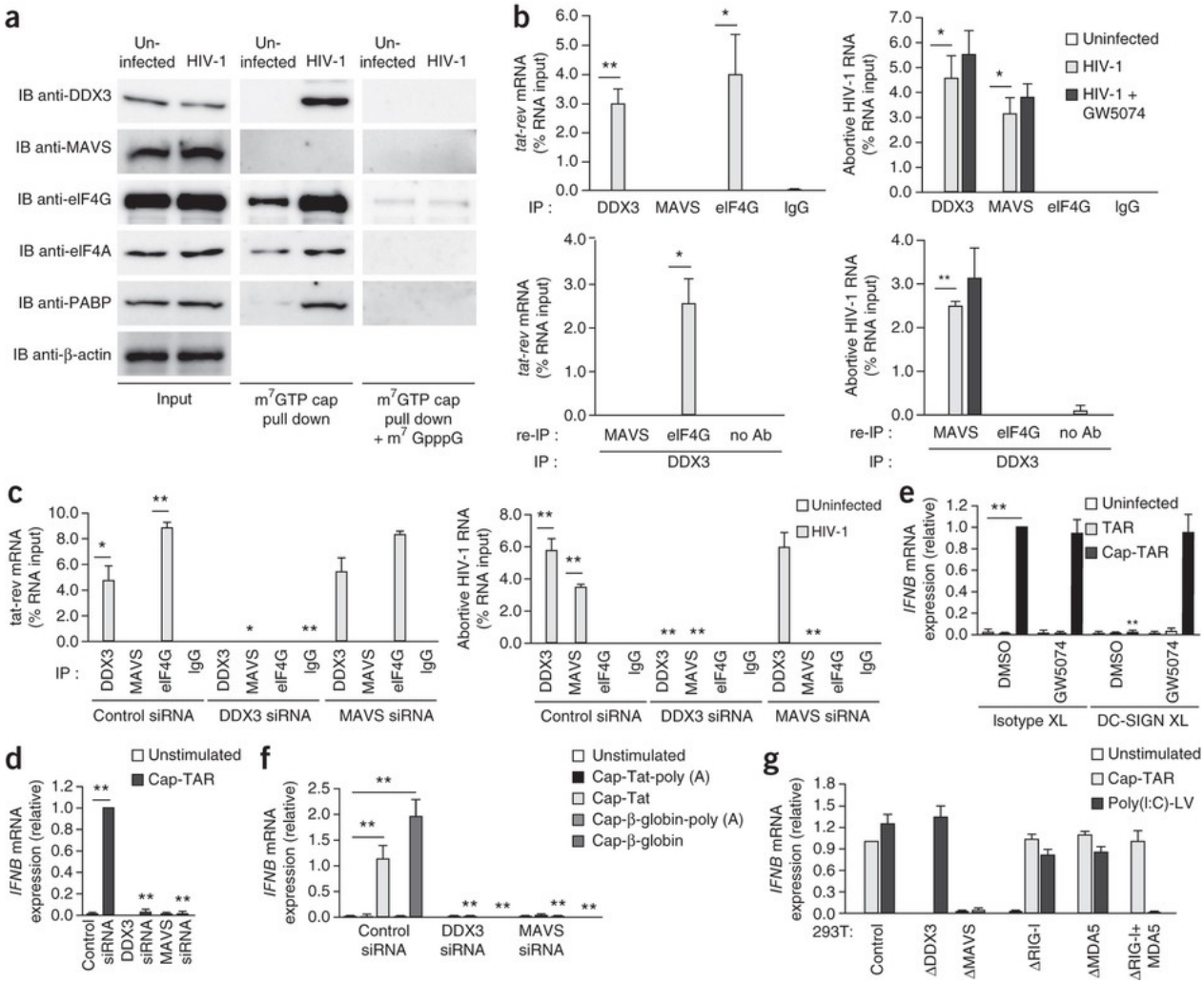
a
Un-infected
HIV-1
IB anti-DDX3
IB anti-MAVS
IB anti-eIF4G
IB anti-eIF4A
IB anti-PABP
IB anti-β-actin
Input
m7GTP cap pull down
m7GTP cap pull down + m7 GpppG
b
tat-rev mRNA (% RNA input)
IP :
DDX3
MAVS
eIF4G
IgG
Abortive HIV-1 RNA (% RNA input)
Uninfected
HIV-1
HIV-1 + GW5074
re-IP :
no Ab
c
Control siRNA
DDX3 siRNA
MAVS siRNA
e
IFNB mRNA expression (relative)
TAR
Cap-TAR
DMSO
GW5074
Isotype XL
DC-SIGN XL
d
Unstimulated
f
Cap-Tat-poly (A)
Cap-Tat
Cap-β-globin-poly (A)
Cap-β-globin
g
Poly(I:C)-LV
293T:
ΔDDX3
ΔMAVS
ΔRIG-I
ΔMDA5
ΔRIG-I+ MDA5

Figure 4

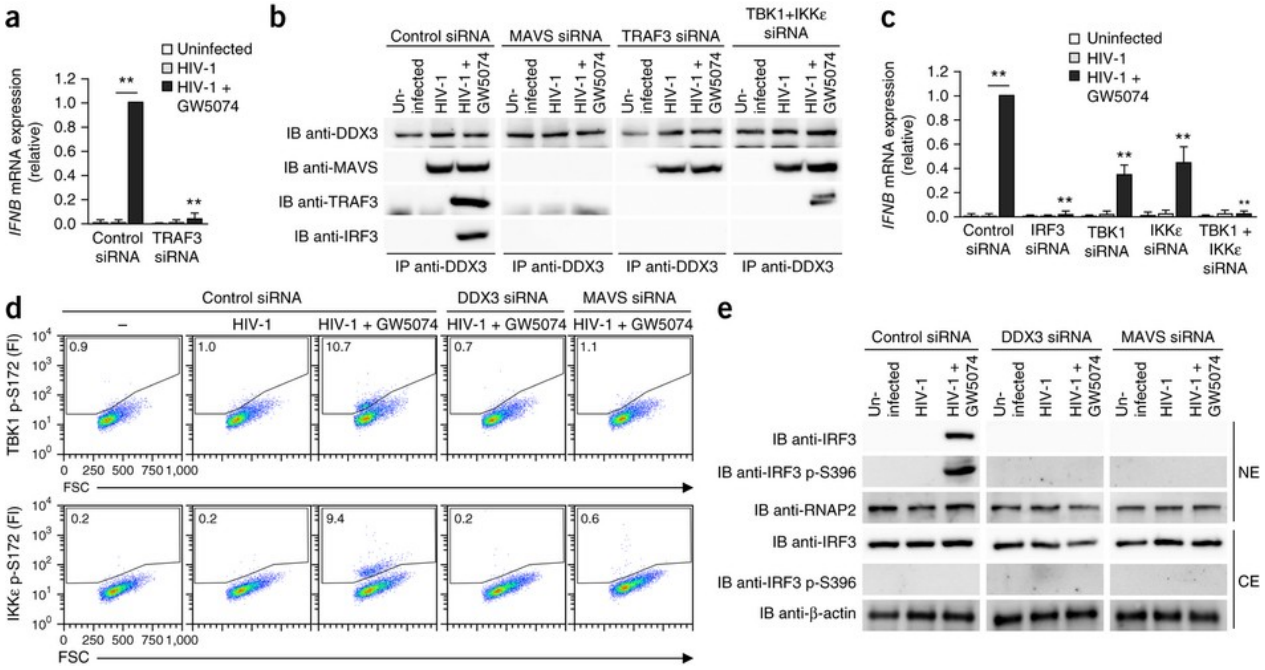
a
Uninfected
HIV-1
HIV-1 + GW5074
IFNB mRNA expression (relative)
Control siRNA
TRAF3 siRNA
b
Control siRNA
MAVS siRNA
TRAF3 siRNA
TBK1+IKKε siRNA
Un-infected
HIV-1
HIV-1 + GW5074
IB anti-DDX3
IB anti-MAVS
IB anti-TRAF3
IB anti-IRF3
IP anti-DDX3
c
Uninfected
HIV-1
HIV-1 + GW5074
IFNB mRNA expression (relative)
Control siRNA
IRF3 siRNA
TBK1 siRNA
IKKε siRNA
TBK1 + IKKε siRNA
d
Control siRNA
DDX3 siRNA
MAVS siRNA
–
HIV-1
HIV-1 + GW5074
TBK1 p-S172 (FI)
IKKε p-S172 (FI)
FSC
e
Control siRNA
DDX3 siRNA
MAVS siRNA
Un-infected
HIV-1
HIV-1 + GW5074
IB anti-IRF3
IB anti-IRF3 p-S396
IB anti-RNAP2
IB anti-β-actin
NE
CE

Figure 5

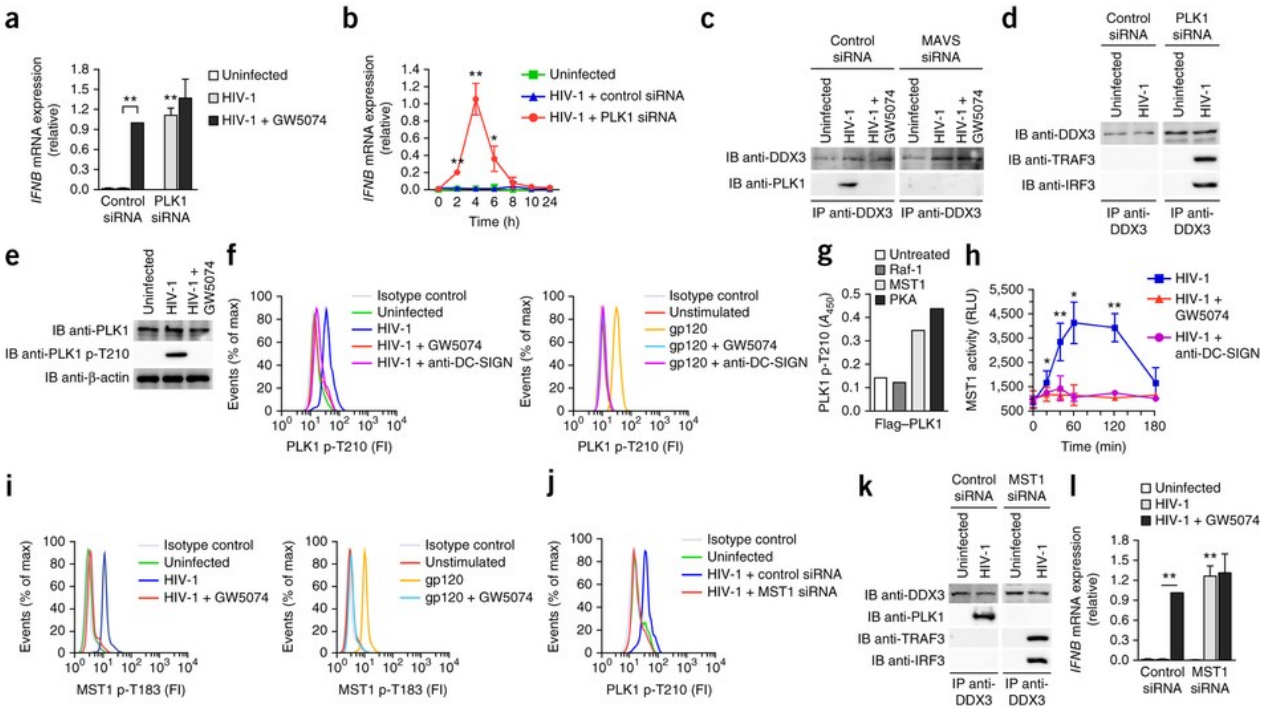
a
IFNB mRNA expression (relative)
Uninfected
HIV-1
HIV-1 + GW5074
Control siRNA
PLK1 siRNA
b
IFNB mRNA expression (relative)
Uninfected
HIV-1 + control siRNA
HIV-1 + PLK1 siRNA
Time (h)
c
Control siRNA
MAVS siRNA
IB anti-DDX3
IB anti-PLK1
IP anti-DDX3
d
Control siRNA
PLK1 siRNA
IB anti-DDX3
IB anti-TRAF3
IB anti-IRF3
IP anti-DDX3
e
IB anti-PLK1
IB anti-PLK1 p-T210
IB anti-β-actin
f
Isotype control
Uninfected
HIV-1
HIV-1 + GW5074
HIV-1 + anti-DC-SIGN
Events (% of max)
PLK1 p-T210 (FI)
Unstimulated
gp120
gp120 + GW5074
gp120 + anti-DC-SIGN
g
Untreated
Raf-1
MST1
PKA
PLK1 p-T210 (A450)
Flag–PLK1
h
HIV-1
HIV-1 + GW5074
HIV-1 + anti-DC-SIGN
MST1 activity (RLU)
Time (min)
i
MST1 p-T183 (FI)
j
HIV-1 + control siRNA
HIV-1 + MST1 siRNA
k
MST1 siRNA
l

Figure 6

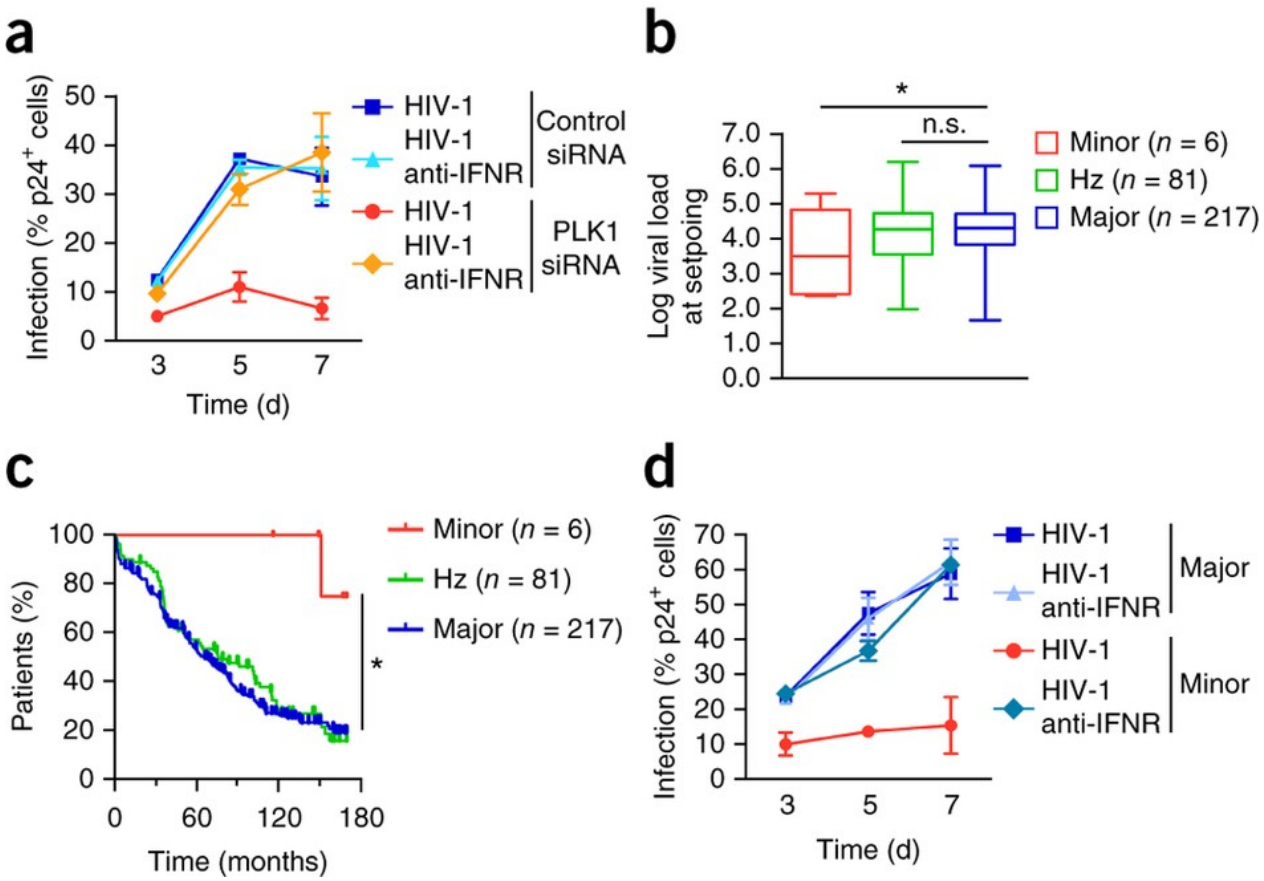
a
Infection (% p24+ cells)
50
40
30
20
10
0
3
5
7
Time (d)
HIV-1
HIV-1 anti-IFNR
Control siRNA
HIV-1
HIV-1 anti-IFNR
PLK1 siRNA
b
*
n.s.
Log viral load at setpoing
7.0
6.0
5.0
4.0
3.0
2.0
1.0
0.0
Minor (n = 6)
Hz (n = 81)
Major (n = 217)
c
Patients (%)
100
80
60
40
20
0
0
60
120
180
Time (months)
Minor (n = 6)
Hz (n = 81)
Major (n = 217)
*
d
Infection (% p24+ cells)
70
60
50
40
30
20
10
0
3
5
7
Time (d)
HIV-1
HIV-1 anti-IFNR
Major
HIV-1
HIV-1 anti-IFNR
Minor

Figure 7

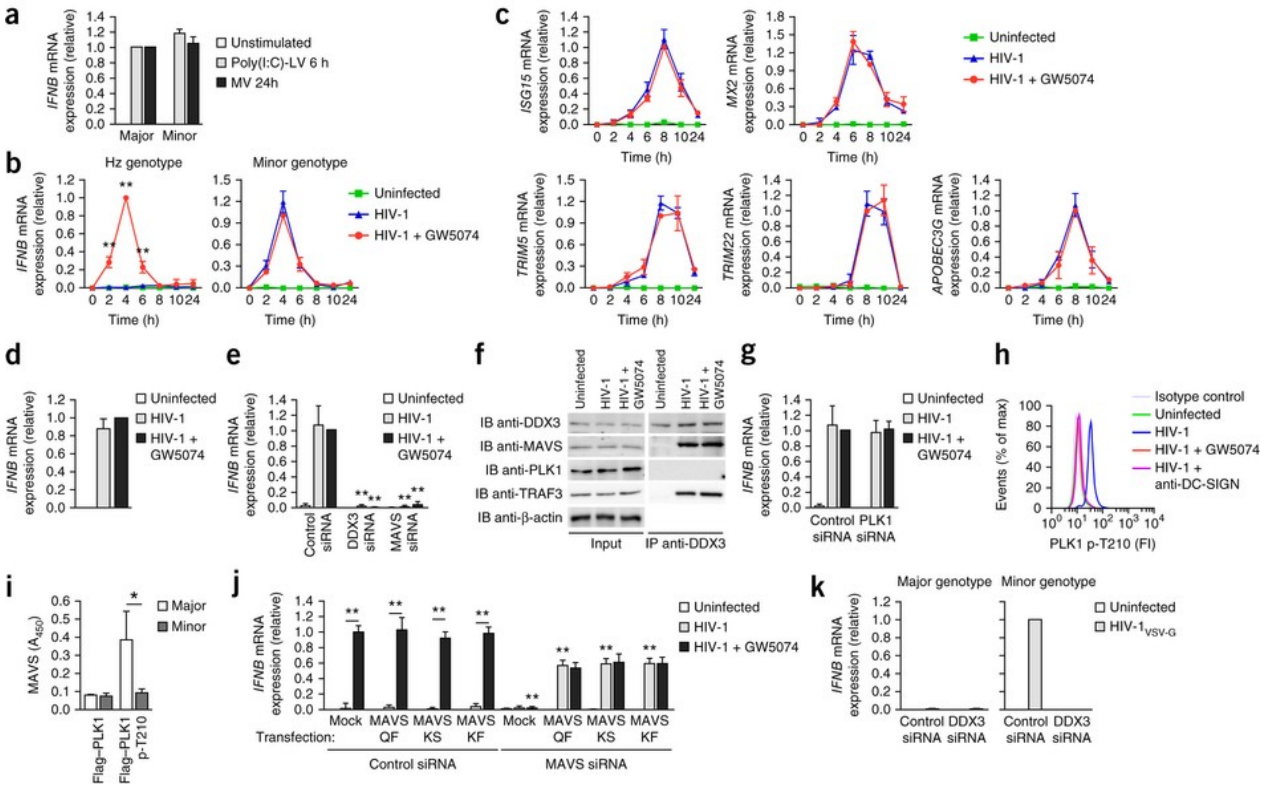
a
IFNB mRNA expression (relative)
Unstimulated
Poly(I:C)-LV 6 h
MV 24h
Major Minor
b
Hz genotype
Minor genotype
IFNB mRNA expression (relative)
Time (h)
Uninfected
HIV-1
HIV-1 + GW5074
c
ISG15 mRNA expression (relative)
MX2 mRNA expression (relative)
TRIM5 mRNA expression (relative)
TRIM22 mRNA expression (relative)
APOBEC3G mRNA expression (relative)
Time (h)
Uninfected
HIV-1
HIV-1 + GW5074
d
IFNB mRNA expression (relative)
Uninfected
HIV-1
HIV-1 + GW5074
e
IFNB mRNA expression (relative)
Control siRNA
DDX3 siRNA
MAVS siRNA
f
Uninfected
HIV-1
HIV-1 + GW5074
IB anti-DDX3
IB anti-MAVS
IB anti-PLK1
IB anti-TRAF3
IB anti-β-actin
Input
IP anti-DDX3
g
IFNB mRNA expression (relative)
Control siRNA
PLK1 siRNA
h
Events (% of max)
PLK1 p-T210 (FI)
Isotype control
Uninfected
HIV-1
HIV-1 + GW5074
HIV-1 + anti-DC-SIGN
i
MAVS (A450)
Major
Minor
Flag–PLK1
Flag–PLK1 p-T210
j
IFNB mRNA expression (relative)
Uninfected
HIV-1
HIV-1 + GW5074
Transfection:
Mock
MAVS QF
MAVS KS
MAVS KF
Control siRNA
MAVS siRNA
k
Major genotype
Minor genotype
IFNB mRNA expression (relative)
Uninfected
HIV-1VSV-G
Control siRNA
DDX3 siRNA

Figure 8

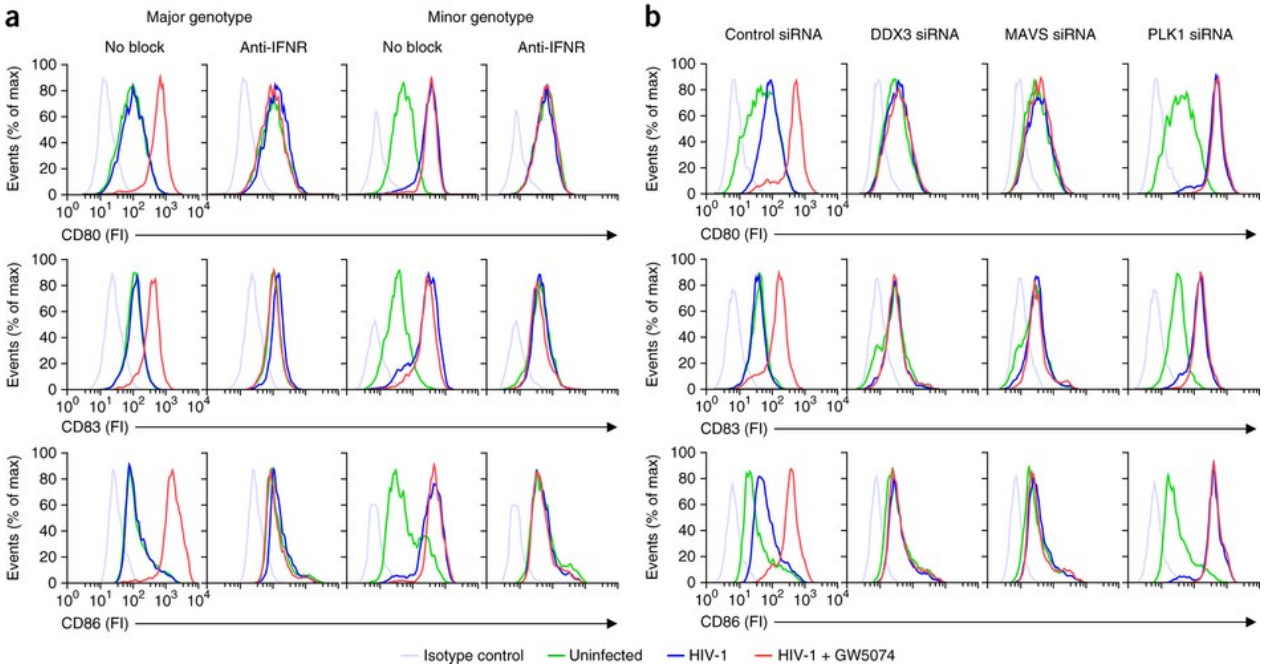
a
Major genotype
Minor genotype
No block
Anti-IFNR
No block
Anti-IFNR
b
Control siRNA
DDX3 siRNA
MAVS siRNA
PLK1 siRNA
Events (% of max)
CD80 (FI)
CD83 (FI)
CD86 (FI)
Isotype control
Uninfected
HIV-1
HIV-1 + GW5074

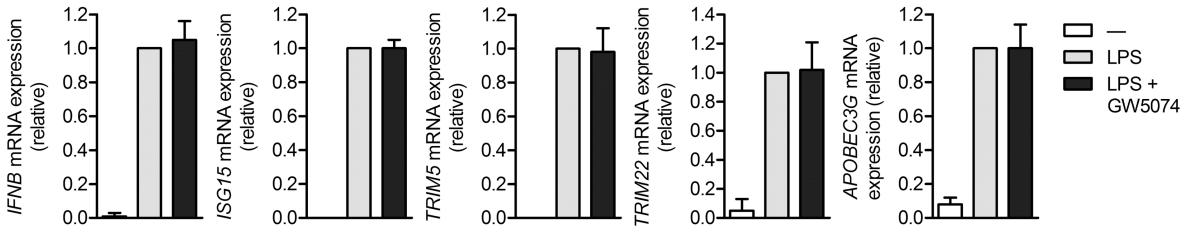

Supplementary Figure 1

Raf-1 inhibition does not affect TLR4-induced type I IFN responses.

Real-time PCR analyses of IFNB, ISG15, TRIM5, TRIM22 and APOBEC3G mRNA in moDCs 6 h after stimulation with TLR4 ligand LPS, in the absence or presence of Raf inhibitor GW5074. Mean ± SD; n = 3.

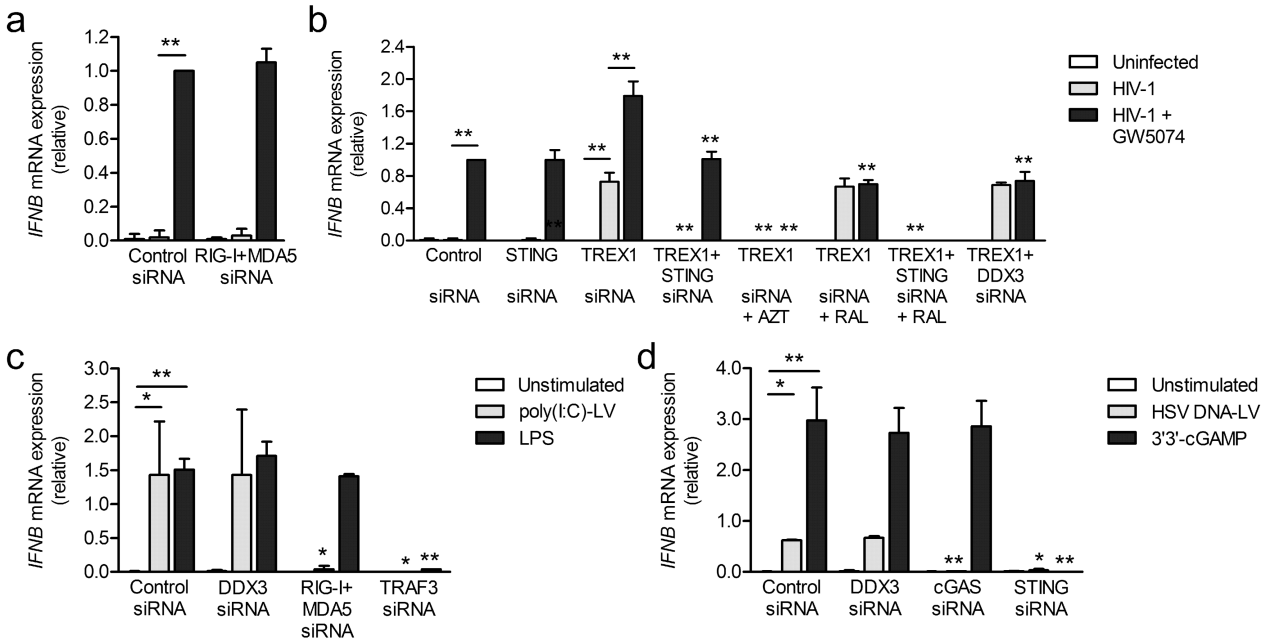

Supplementary Figure 2

DDX3 sensing pathway is independent from RIG-I/MDA5 and cGAS pathways in DCs.

(**a-d**) Real-time PCR analyses of *IFNB* mRNA in moDCs 4 h after infection with HIV-1_{BaL} (**a,b**) or stimulation with RIG-I-MDA5 ligand poly(I:C)-LyoVec, TLR4 ligand LPS (**d**), cGAS ligand HSV DNA coupled to LyoVec or STING ligand 3'3'-cGAMP (**d**), in the absence or presence of Raf inhibitor GW5074 (**a,b**), reverse transcription inhibitor AZT or integrase inhibitor raltegravir (RAL) (**b**) and after silencing (siRNA) of indicated proteins (**a-d**). Mean ± SD; n = 4 (**a,c,d**), 3 (**b**). ** $p < 0.01$, * $p < 0.05$ (Student's *t*-test). The data shown in (**b**) are an addendum to the data presented in **Fig. 2b**.

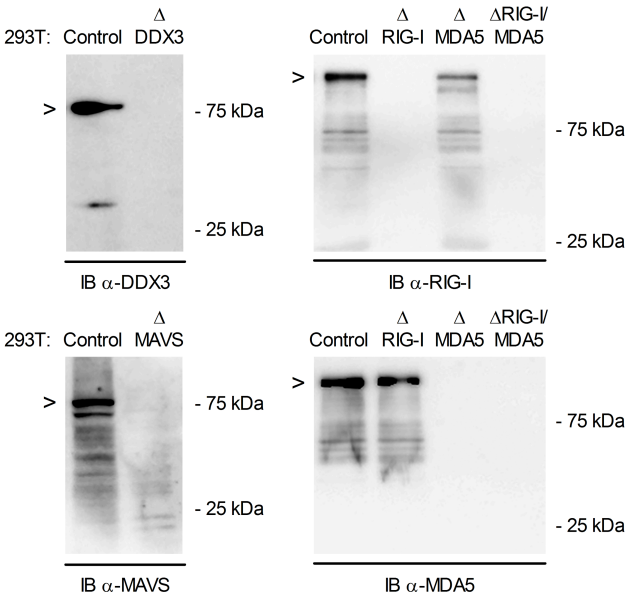

Supplementary Figure 3

Depletion of protein expression in human 293T cells by CRISPR/Cas9-directed genome editing

Immunooblot analyses of depletion (Δ) of indicated proteins by transfection of 293T cells with control or specific guide RNA and Cas9-expressing plasmids.

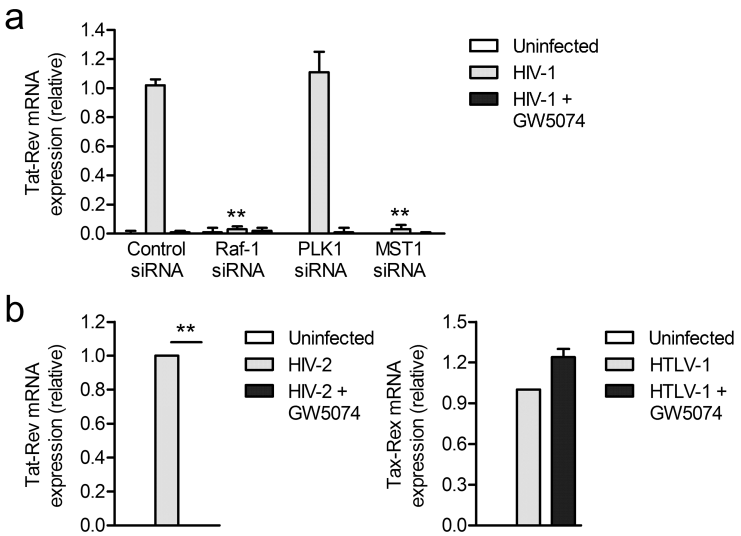

Supplementary Figure 4

Raf-1 and MST1 but not PLK1 inhibit HIV-1 transcription, while Raf-1 blocks HIV-2 but not HTLV-1 transcription.

(a,b) Real-time PCR analyses of Tat-Rev (HIV-1, HIV-2) or Tax-Rex (HTLV-1) mRNA in moDCs 6 h after infection with HIV-1BaL (a), HIV-2 or HTLV-1 (b), in the absence or presence of Raf inhibitor GW5074 (a,b), and after silencing (siRNA) of indicated proteins (a). silenced for Raf-1, PLK1 or MST1 by RNAi after 6 h infection. Mean ± SD; n = 6 (a), 2 (b).

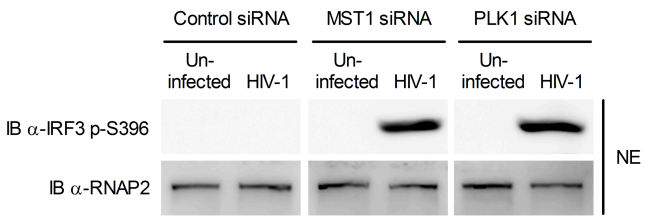

Supplementary Figure 5

IRF3 activation is suppressed by a MST1-PLK1 cascade after HIV-1 infection.

Immunoblot (IB) analyses of Ser396 phosphorylation of IRF3 in nuclear extracts (NE) of moDCs 3 h after HIV-1BaL infection, after silencing (siRNA) of MST1 or PLK1. RNA polymerase II (RNAP2) served as loading control. Representative of 2 independent experiments.

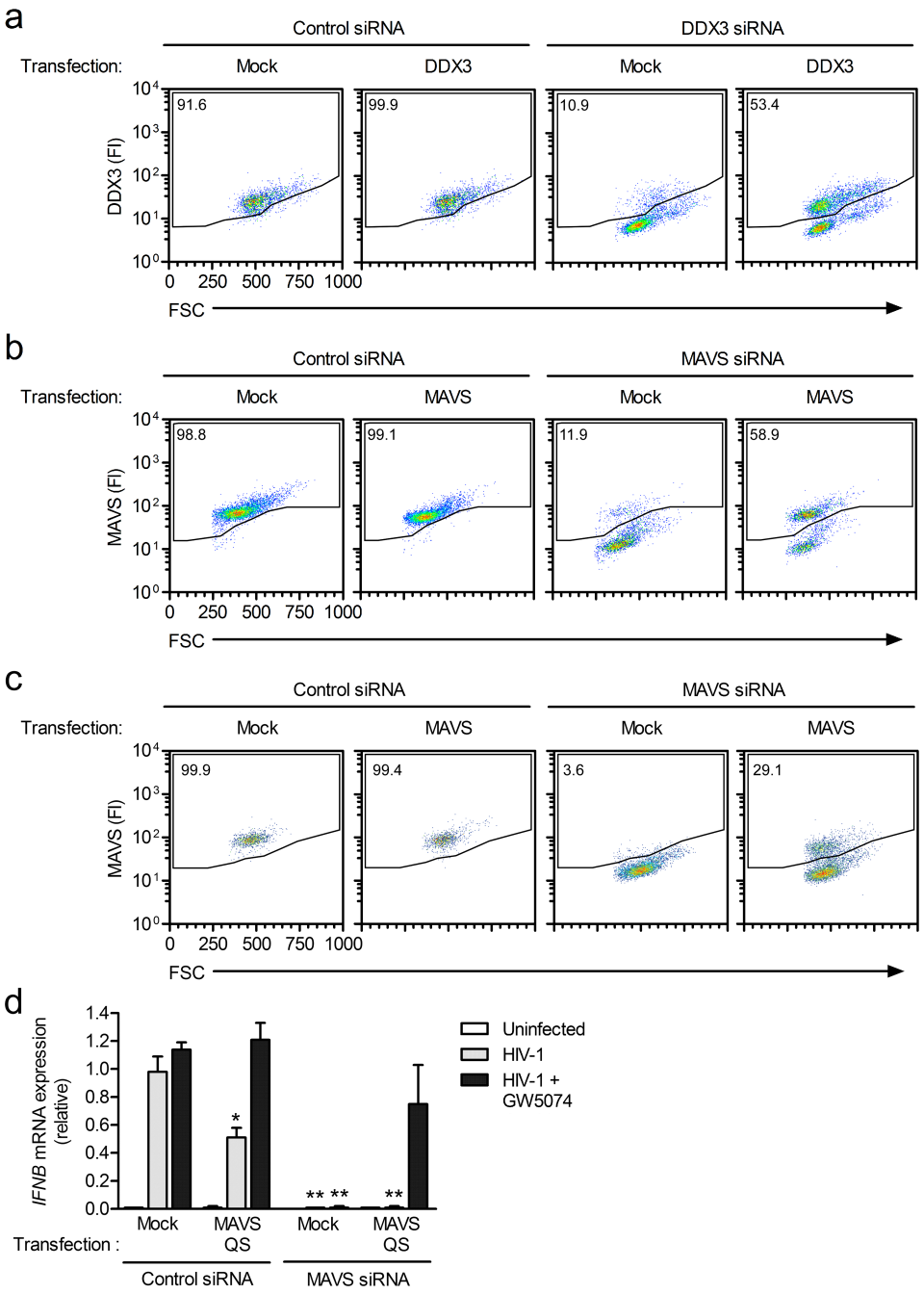

Supplementary Figure 6

Rescue of DDX3 or MAVS expression in moDCs after silencing restores type I IFN responses after HIV-1 infection.

(a-c) Flow cytometry analyses of DDX3 (a) or MAVS (b,c) expression in control-, DDX3- or MAVS-silenced (siRNA) moDCs 48 h after transfection of plasmids with RNAi-resistant cDNAs encoding wild-type DDX3 (a) or wild-type MAVS (b,c). In (c), minor genotype moDCs were transfected. FI, fluorescence intensity; FSC, forward scatter. Representative of 4 (a,b) or 3 (c) independent experiments. (d) Real-time PCR analyses of IFNB mRNA in control- or MAVS-silenced minor genotype moDCs 4 h after infection with HIV-1BaL, in the absence or presence of Raf inhibitor GW5074, after complementation of MAVS expression via transfection of plasmids with RNAi-resistant cDNA encoding wild-type (QS, Q198/S409) MAVS. Mean ± SD; n = 4. ** $p < 0.01$, * $p < 0.05$ (Student's t-test).

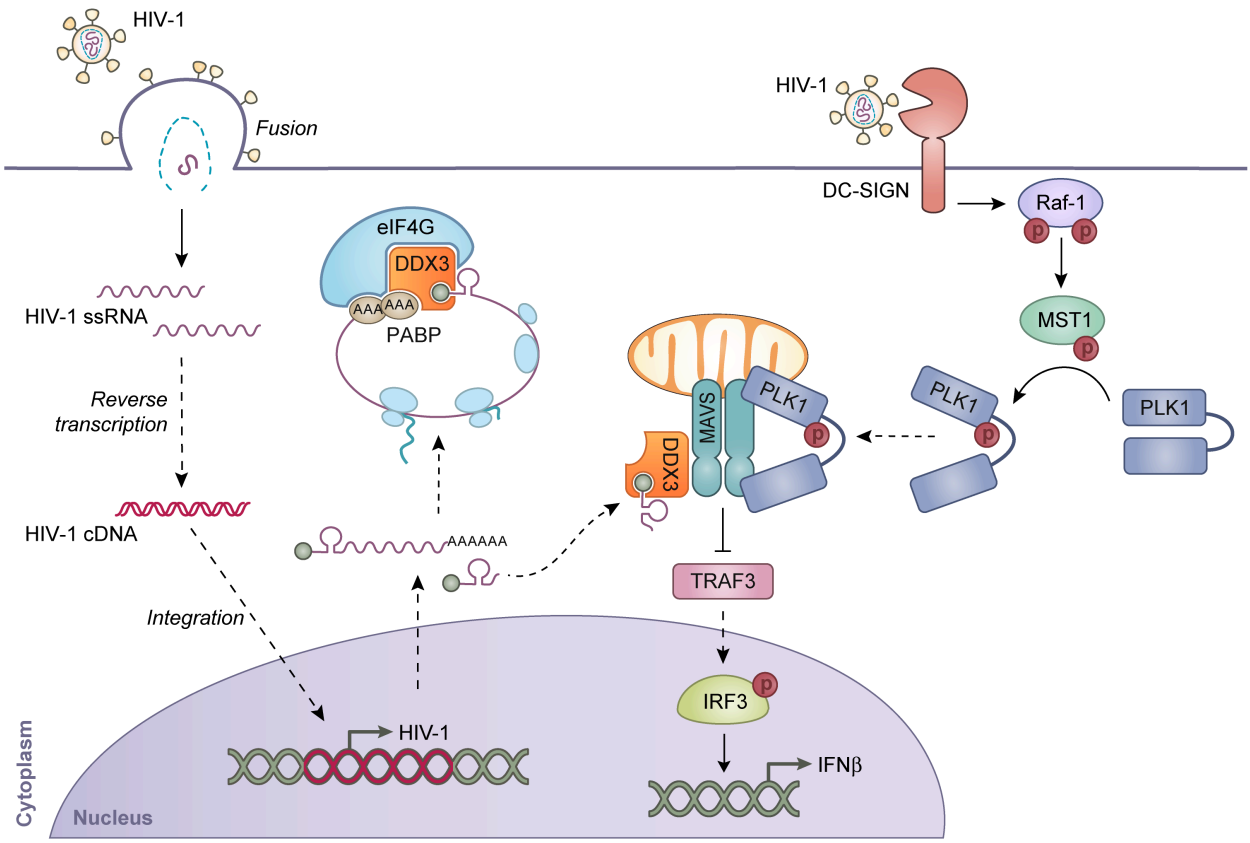

Supplementary Figure 7

DC-SIGN signaling via Raf-1-MST1-PLK1 suppresses signaling downstream of MAVS after sensing of abortive HIV-1 transcripts by RNA helicase DDX3.

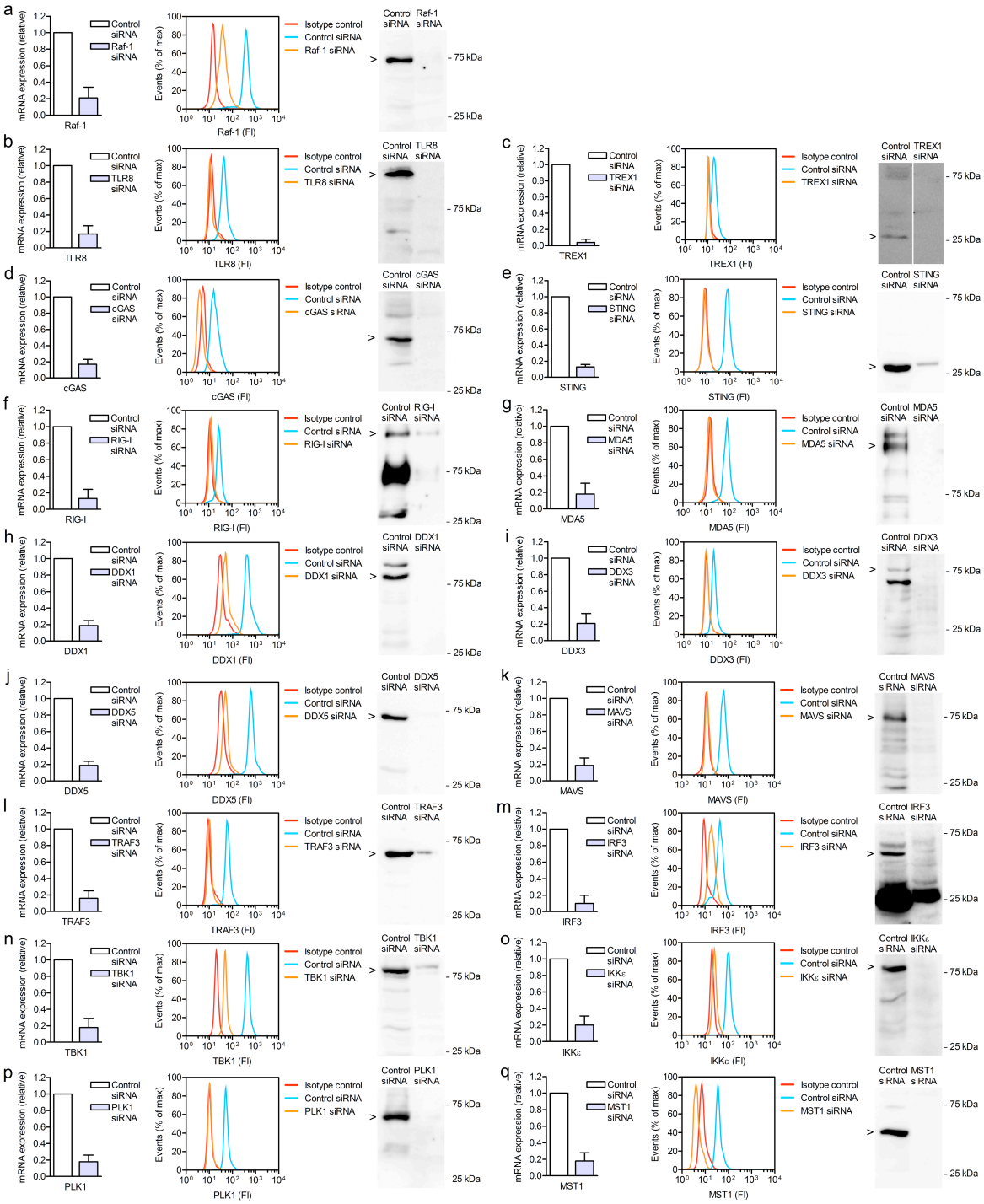

Supplementary Figure 8

Silencing of protein expression in human DCs by RNA interference.

(a-q) Realtime PCR (left panels), flow cytometry (middle panels) and immunoblot (right panels) analsyes of indicated mRNA and proteins in moDCs silenced for indicated proteins using specific siRNAs and non-targeting siRNA as a control (left panels; mean ± SD, n ≥ 7; middle panels; FI, fluorescence intensity; representative of at least 3 independent experiments; right panels; representative of 2 independent experiments).

RNA	Sequence
HIV-1 TAR	GGTCTCTCTGGTTAGACCAGATCTGAGCCTGGGAGCTCTCTGGCTAACTAGGGAACCC
HIV-1 Tat	GGTCTCTCTGGTTAGACCAGATCTGAGCCTGGGAGCTCTCTGGCTAACTAGGGAACCCACT GCTTAAGCCTCAATAAAGCTTGCCTTGAGTGCTCAAAGTAGTGTGTGCCCGTCTGTTGTGTG ACTCTGGTAACTAGAGATCCCTCAGACCCTTTTAGTCAGTGTGGAAAATCTCTAGCAGTGGC GCCCGAACAGGGACTTGAAAGCGAAAGTAAAGCCAGAGGAGATCTCTCGACGCAGGACTCG GCTTGCTGAAGCGCGCACGGCAAGAGGCGAGGGGCGGCGACTGAATTGGGTGTCGACATA GCAGAATAGGCGTTACTCGACAGAGGAGAGCAAGAAATGGAGCCAGTAGATCCTAGACTAG AGCCCTGGAAGCATCCAGGAAGTCAGCCTAAAACTGCTTGTACCAATTGCTATTGTAAAAAGT GTTGCTTTCATTGCCAAGTTTGTTTCATGACAAAAGCCTTAGGCATCTCCTATGGCAGGAAGA AGCGGAGACAGCGACGAAGAGCTCATCAGAACAGTCAGACTCATCAAGCTTCTCTATCAAAG CAACCCACCTCCCAATCCCGAGGGGACCCGACAGGCCCGAAGGAATAGAAGAAGAAGGTG GAGAGAGAGACAGAG
β-globin	ACATTTGCTTCTGACACAACTGTGTTCACTAGCAACCTCAAACAGACACCATGGTGCATCTGA CTCCTGAGGAGAAGTCTGCCGTTACTGCCCTGTGGGGCAAGGTGAACGTGGATGAAGTTGG TGGTGAGGCCCTGGGCAGGCTGCTGGTGGTCTACCCTTGGACCCAGAGGTTCTTTGAGTCC TTTGGGGATCTGTCCACTCCTGATGCTGTTATGGGCAACCCTAAGGTGAAGGCTCATGGCAA GAAAGTGCTCGGTGCCTTTAGTGATGGCCTGGCTCACCTGGACAACCTCAAGGGCACCTTT GCCACACTGAGTGAGCTGCACTGTGACAAGCTGCACGTGGATCCTGAGAACTTCAGGCTCC TGGGCAACGTGCTGGTCTGTGTGCTGGCCCATCACTTTGGCAAAGAATTCACCCCACCAGTG CAGGCTGCCTATCAGAAAGTGGTGGCTGGTGTGGCTAATGCCCTGGCCCACAAGTATCACT AAGCTCGCTTTCTTGCTGTCCAATTTCTATTAAAGGTTC

Supplementary Table 1 RNA sequences used for LyoVec-mediated transfection.

Gene product	Forward primer	Reverse primer
GAPDH	CCATGTTCGTCATGGGTGTG	GGTGCTAAGCAGTTGGTGGTG
IFNβ	ACAGACTTACAGGTTACCTCCGAAAC	CATCTGCTGGTTGAAGAATGCTT
ISG15	TTTGCCAGTACAGGAGCTTGTG	GGGTGATCTGCGCCTTCA
Mx2	ACTGAAAAAGCAGCCCTGTGA	ATGACGTTCTGGGCTTTGTGTAT
Trim5α	AGAACATACGGCCTAATCGGC	CAACTTGACCTCCCTGAGCTTC
Trim22	CTGTGCCTCCCTGTCGTATTG	GAGTGCTCCGTGGTTTGTGAC
APOBEC3G	TTGAGCCTTGGAATAATCTGCC	TCGAGTGTCTGAGAATCTCCCC
Raf-1	GGTGATAGTGGAGTCCCAGCA	TCAGATGAGGGACTGGAGGTG
TREX1	GCAGAGCTGGCTATGCTGG	TCAGCGCAGTGATGCTATCC
cGAS	CTGGCCAACATGGTGAAACC	CAGGCACGTACCACCATGC
STING	TGGCTCCTGGTCATGTTCC	CCCAAACTCAGCCTCCTCC
RIG-I	CCAAGCCAAAGCAGTTTTCAAG	CATGGATTCCCCAGTCATGG
MDA5	TGAGAGCCCTGTGGACAACC	CGCTGCCCACTTAGAGAAGC
DDX1	GCACCTACTGTTCAAGAGTTGGC	AACAGCTGGTTAGGAAGGTAGCC
DDX3	AGTGATTACGATGGCATTGGC	AGCGACTGTTTCCACCACG
DDX5	AGTGGCACAGACTGGATCTGG	GAATGGCTGATGATTGATGTGG
MAVS	TGATTTCCTCGCAATCAGACG	GAAGCCGATTTCCAGCTGTATG
TRAF3	ATCTGCCCGATCCCTGATAAG	AGACAGACCGGTTCAAATCCC
IRF3	AAGGAGGCGTGTTTGACCTG	CATAGCGTGGTGAGCGTCC
TBK1	TTACAGGAAAGCCTTCTGGTGC	TCCACTCCAGTCAATTGGTCC
IKKε	TTGGAGTGACCTTGTACCATGC	CATGATCTCCTTGTTCCGCC
PLK1	TGGTTCGAGAGACAGGTGAGG	AGGCATTGACACTGTGCAGC
MST1	TGCCATGGACTCAACACTCG	TCATGATGCAGGTCCGTACG
HIV-1 Tat-Rev	ATGGCAGGAAGAAGCGGAG	ATTCCTTCGGGCCTGTCG
HIV-1 abortive RNA	GGGTCTCTCTGGTTAGACCAGATC	GGTTCCCTAGTTAGCCAGAGAGC
HIV-2 Tat-Rev	AATGTTGCTACCATTGCCAGC	TGGATACGGATTTGTCTGATGC
HTLV-1 Tax-Rex[1]	ATCCCGTGGAGACTCCTCAA	AACACGTAGACTGGGTATCC

Supplementary Table 2 Primer sequences used for real-time PCR analysis.

1. Kinoshita, T. *et al.* Detection of mRNA for the tax1/rex1 gene of human T-cell leukemia virus type I in fresh peripheral blood mononuclear cells of adult T-cell leukemia patients and viral carriers by using the polymerase chain reaction. *Proc. Natl. Acad. Sci. U. S. A.* **86**, 5620-5624 (1989).